MOLECULAR BASIS OF MAMMALIAN PRION PROTEIN MISFOLDING

Committee:

Claudio Soto, PhD, Supervisor

Jose Barral, PhD, Chair

Andres Oberhauser, PhD

Giulio Taglialatela, PhD

Claudio Hetz, PhD

Dean, Graduate School

MOLECULAR BASIS OF MAMMALIAN PRION PROTEIN MISFOLDING

by

Rodrigo Diaz Espinoza

Dissertation

Presented to the Faculty of the Graduate School of The University of Texas Medical Branch in Partial Fulfillment of the Requirements for the Degree of

DOCTOR OF PHILOSOPHY

The University of Texas Medical Branch

2011

Dedication

To my parents, for they are the reasons I can write these words: my father, Carlos Diaz Valenzuela, who has been both the inspiration and the lighting spark on my journey into Science, and my mother, Paulina Espinoza Varas, who gave me support, strength and love when I most needed

To my brother and best friend, Diego Diaz Espinoza

To Andrea Garces, for her encouraging feedback, care and love

Acknowledgements

I would like to first thank the members of my dissertation committee, Dr. Andres Oberhauser, Dr. Jose Barral, Dr. Giulio Taglialatela and Dr. Claudio Hetz, who have been very helpful and supportive throughout my thesis.

I also want to show my gratitude to my UTMB's best friends: Jeff Chen, a passionate friend who gave me support and help when I needed; Abhisek Mukherjee, who has been a partner throughout all of my research, and Aditya Hindupur, whose feedback has always been enlightening.

For the great work environment and support they provide every day, I would also like to thank the people in the "Protein Misfolding Laboratory", especially Mohammad Shahnawaz, one of the "lights" in the lab who makes every day better, Marcelo Barria (former member), for his passion about simple things, and Rodrigo Morales, for his help in many projects.

Last but not least, I would like to give my deepest appreciation to Dr. Claudio Soto, whose mentorship has been far beyond experimental-related issues. From him I have learnt, and still learning, several of the most important aspects in science: attitude and "crazy" thinking. His careful listening, flexibility and open-minded reasoning have been crucial for developing the work I present here, and also for ongoing and future projects. Thanks to him and also the people in the lab, the time spent on my research work has been enlightening and joyful.

MOLECULAR BASIS OF MAMMALIAN PRION PROTEIN MISFOLDING

Publication No

Rodrigo Diaz Espinoza, PhD

The University of Texas Medical Branch, 2011

Supervisor: Claudio Soto

Prions are aberrantly folded proteins that are able to self-propagate their abnormal conformation using the normally folded protein as substrate. In mammals, the only known prion protein is PrP. The misfolding of PrP is a key event underlying Transmissible Spongiform Encephalopaties (TSEs), fatal neurological disorders that affect many mammalian species. A self-propagating abnormally folded PrP is believed to be the essential component within the infectious agent, in what is called the protein-only hypothesis. Although the fundamental role of PrP in prion diseases has been settled after many years of research, the structural and mechanistic details of the conversion process leading to the infectious PrP conformation (PrP^{Sc}) is not yet elucidated. Moreover, the structure of the pathogenic entity is unknown and a crucial involvement of accessory molecules within the infectious particle has recently gained strong evidence. Prions have raised not only health-related concerns but also great interest from basic science due to their unusual features as pathogenic infectious agents. In order to gain insights into the molecular aspects featuring the PrP conversion process, I analyzed the role of PrP and

potential accessory molecules on the formation of prion-like molecules. Under close-to-physiological conditions, I found that kosmotropic anions specifically modulate the formation of PrP aggregates with features reminiscent of PrP^{Sc}. I also studied the role of accessory molecules known to affect the conversion process. I found that the protease resistance of PrP aggregates, a well known biochemical hallmark of PrP^{Sc}, was highly dependent on the presence of hydrophobic and negatively charged molecules. Altogether, the results provide evidence toward the idea that the formation of prions is a synergistic event in which both PrP and accessory molecules are fundamental components.

Table of Contents

List of Figures

List of Tables

CHAPTER 1

INTRODUCTION

1.1 PRION DISEASES

Transmissible Spongiphorm Encephalopaties (TSEs) are fatal and infectious neurological maladies in mammals caused by an atypical infectious agent termed "prion". It was originally described as a contagious disease under the name of "*scrapie*" which causes devastating motor problems in sheep[1]. Later on, similar manifestations of symptoms started to be recognized in other diseases such as "*Kuru*", one of the human versions of prion diseases[2]. The failures associated to the isolation of the infectious agent using conventional techniques aimed to identify bacteria, viruses and other known pathogenic entities brought great interest from the scientific community[3]. In the 90's, an outbreak of prion diseases in cows destined for human consume raised national alarms with the confirmation of several cases of prion-disease-infected humans. From the pathological point of view, prion diseases are generally characterized by relatively long incubation periods, extreme vacuolation in specific regions of the brains, serious motor impairments and general neuronal degeneration. All prion-related diseases are fatal and no cure has been so far developed.

1.2 MOLECULAR NATURE OF PRIONS

The difficulties in identifying the infectious agent underlying prion diseases, added to the unusually high resistance to radiation, heat and other conventional sterilization techniques, led John Griffith to the proposal that the prion agent is a self-propagating protein in an abnormal

conformation, in what was later called the "*protein only hypothesis*"[4] . The isolation of a protein fraction from scrapie-infected animal brains that co-purified with infectivity enabled the identification of a new protein termed PrP (*prion protein*), a glycosylated, GPI-anchored lipid membrane protein that is mainly expressed in the brain [5, 6] (Fig. 1.1). Further experiments showing the absolute resistance to prion infection of PrP knock-out mice finally settled the essential involvement of PrP in the disease[7]. In addition, large depositions of PrP in the form of aggregates are typically observed in the brains of diseased animals[8]. These aggregates usually exhibit structural features associated to "*amyloids*", highly organized supra-molecular arrangements of aggregated proteins with high content of b-sheets in their secondary structure[9-13]

.

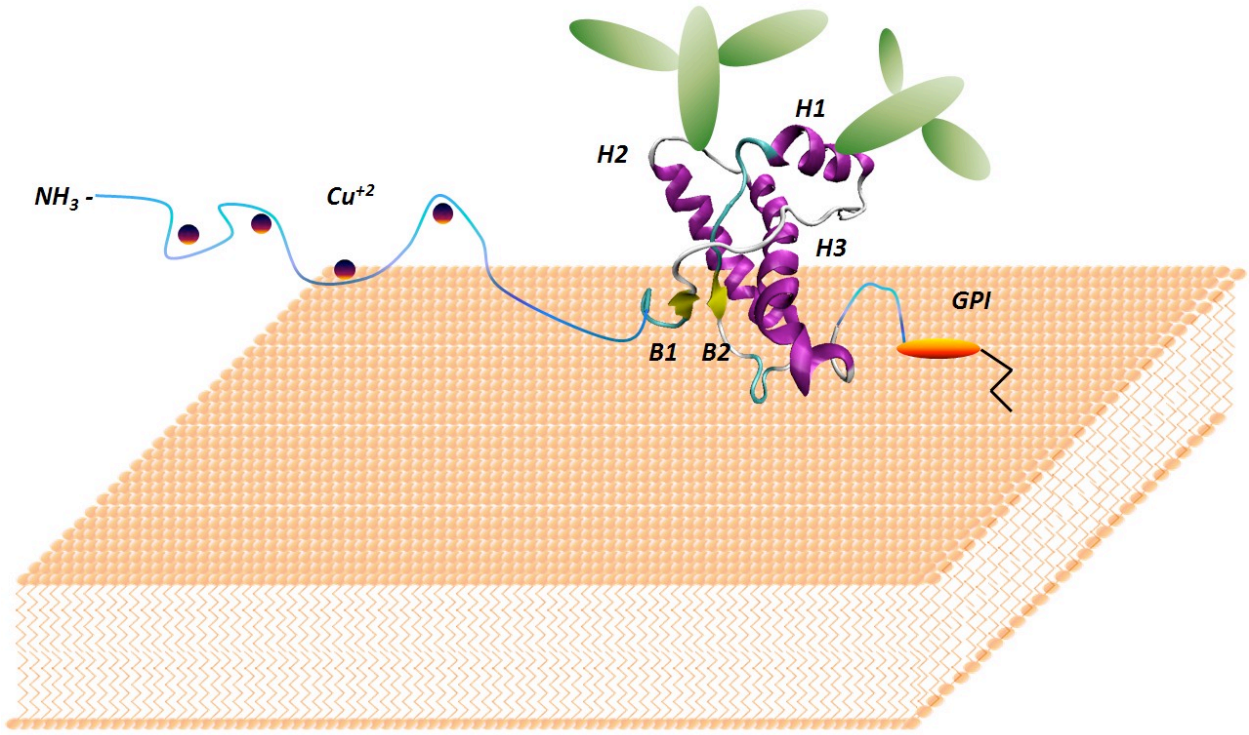

Figure 1.1*: Prion protein at the cell surface.* The 3D structure of PrP is represented in the di-glycosylated form and attached to the cell membrane though a GPI anchor [14, 15]. The N-terminal natively unfolded domain is depicted in blue with copper ions bound to PrP highly basic N-

terminal four octarepeats. Helical regions (H1, H2 and H3) are colored purple whereas b-strands (B1 and B2) are shown in yellow.

The currently accepted view about prions states that the infectious agent is primarily composed of an aberrantly folded (*misfolded*) PrP in its prion state (PrP^{Sc}), which acquires self-propagation features to induce the transformation of the normal PrP conformation (PrP^{C}) into the infectious form [16]. The potential mechanism involved in prion propagation *in vivo* is believed to be dependent of nucleation-polymerization[17]. This mechanism proposes that small "*seeds*" composed of the misfolded protein are able to recruit and convert normally folded proteins in a process called nucleation. When a critical concentration of these nucleuses is reached, amyloid fibrils start to grow and the system goes into elongation phase until most protein substrate is converted [12, 17, 18].

Another intriguing feature of prions is the existence of different "*strains*" that as in the case of viruses represent alternative variations of the agent [19-22]. As in other infectious diseases, these prion strains are usually associated to different pathological phenotypes[22-24]. Biochemical differences on PrP^{Sc} can also be observed between strains [5, 25]. The fact that the same PrP sequence can lead to a diversity of different prion strains have led some to postulate that differences in prion protein conformation underlie the strain phenomenon[26, 27]. Others have proposed that accessory molecules modulate the strain repertoire of a prion[28], or even that a yet unidentified nucleic acid is responsible for the strain properties[29, 30] . Different PrP species also exhibit differential susceptibilities to prion diseases, a phenomenon known as species barrier[31, 32]. Some species are highly compatible and others are virtually impossible to cross-infect. It is thought that species barrier is mainly controlled by the PrP sequence, though some other molecular components interacting with PrP or "co-factors" have also been proposed [28].

In vitro experiments using brain extracts from infected and uninfected animals have shown that it is possible to harvest prions in the test tube and recapitulate most of the biochemical and pathological events by the so-called PMCA (protein misfolding cyclic

amplification) approach [33, 34]. This technique consists of cycles of amplification and sonication that allow the replication and amplification of small prion seeds, providing indirect evidence that prion replicate through the nucleation-polymerization mechanism described above. Despite these great advances, understanding the molecular details of the protein conversion mechanism requires experimental setups relying on pure and defined components mimicking most of the features associated to prion formation. Experiments using exclusively recombinant PrP (recPrP) have so far failed to show infectivity in wild-type animals in a first passage [35, 36]. However, highly infectious synthetic prions have been reported using mixtures of recPrP, lipids and mouse-extracted RNA molecules submitted to PMCA [37]. RecPrP aggregates with highly heterogeneous infectivity were also achieved using modified PMCA experiments using reactions containing recPrP and mixtures of detergents (SDS and triton) [38, 39]. The lack of transmissibility of exclusively protein-only inoculates suggest that accessory co-factor molecules may be essential for prion infectivity in mammals [40, 41].

1.3 RATIONALE OF THE STUDY

1.3.1. Background Problem

Although much study has been conducted to understand the biochemical aspects of prion diseases, the molecular conversion mechanism and the structural details of the prion particles remain elusive. This is mostly due to the physical properties of this unconventional infectious agent, such as insolubility and heterogeneity, which make it virtually intractable for classical biophysical techniques [25]. *In vitro* conversion systems and computational approaches emerge as an alternative and indirect way of studying the phenomenon. In addition, more state-of-the-art structural approaches such as solid-state NMR and spin-labeling assays may overcome some of the difficulties in elucidating the molecular nature of prions[42, 43].

A key question in the field is whether the prion co-factors are needed for prion replication. If so, the question is whether these molecules are involved in the initial misfolding event and/or remains bound to the prion protein in its misfolded state as a necessary prosthetic-

like group, or they only act as accelerators of a reaction that is intrinsically coded within PrP structure and sequence (Fig. 1.2). In addition, co-factors may also be implicated in the prion strain determination as mentioned above. The role of these accessory molecules have recently raised great interest from the scientific community due to the multiples failures in generating *bona fide* prions using protein-only material[35, 36]. The fact that many other amyloid-associated diseases such as Alzheimer's and Parkinson diseases are traditionally considered non-infectious diseases strengthens the idea that co-factors may play a key role in transmissibility of prions. A detailed study of the role and identity of co-factors has not yet been reported.

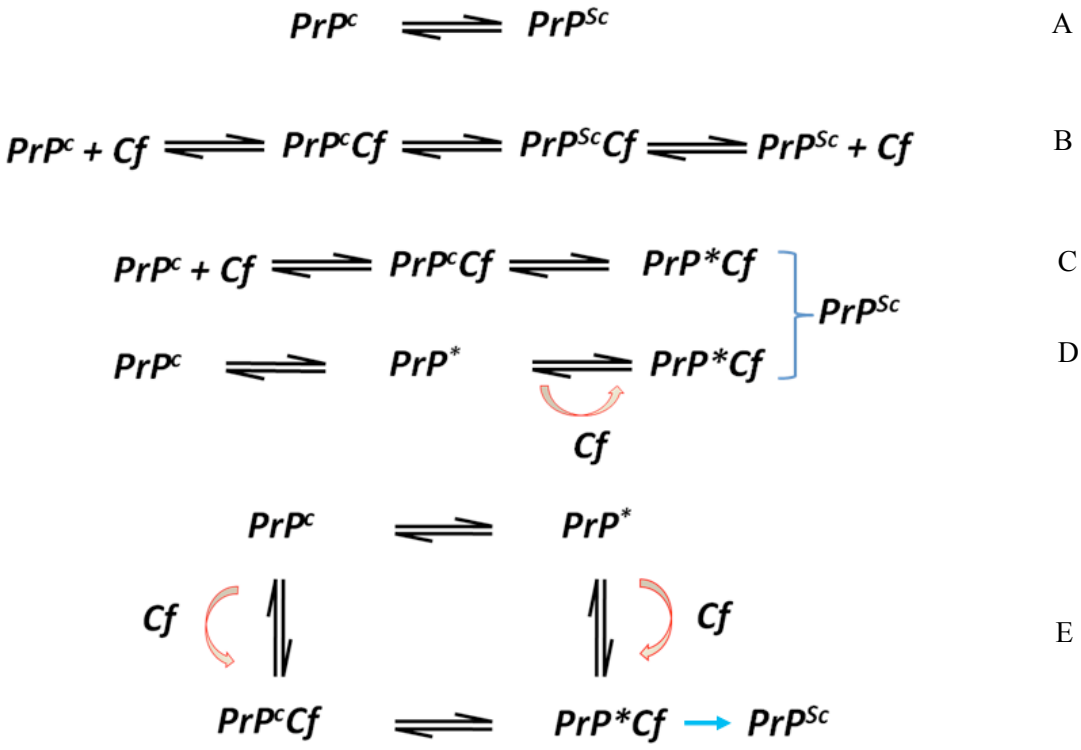

Figure 1.2: *Chemical background for the potential role of co-factors during prion formation.* The protein only hypothesis postulates that an abnormally folded PrP (PrP^{Sc}) acquires self-propagating capabilities and therefore infectivity[4]. Co-factor molecules are shown as Cf. PrP* represents a misfolded PrP without any bound co-factor molecule. A) The simplest possible chemical scenario for the protein only hypothesis. B) An enzyme-like role for the co-factor in a

catalyzed conversion reaction. C) The co-factor, once bound to PrP, induces the conformational change but remains bound to PrP in order to form a bona fide prion particle (PrP^{Sc}). D) A conformational change into PrP* does not require co-factors but the infectious properties of PrP arise when an accessory molecule binds PrP*. E) A combined scenario between C) and D) provides two alternatives pathways to form PrP^{Sc}.

1.3.2. Central hypothesis

Based on the current experimental evidence about prion formation, ***my working hypothesis is that prion propagation is determined by the primary structure of PrP and dependent on accessory molecules that modulate the process***.

In order to test the hypothesis, two aims were designed:

1- *Conversion and misfolding of recombinant PrP in the absence of organic co-factors*.

Typical conversion protocols of recombinant PrP into prion-like forms reported in the literature rely on far-from-physiological experimental setups and extreme conditions. I have designed an experimental approach to modulate the misfolding of recombinant PrP only by adding specific concentrations of kosmotropic salts in a more physiological conversion system. This aim will test the effectiveness of a cofactor-less environment in producing prion-like recombinant PrP aggregates.

2- *Conversion and misfolding of recombinant PrP in the presence of organic co-factors*.

Based on reported experimental protocols to convert recombinant PrP into prion-like forms, I studied the effect of different non-PrP organic molecules on the modulation of the prion-like features and their role in infectivity. These studies are aimed to provide support that accessory molecules convey a primary role in the misfolding process of PrP.

CHAPTER 2

MATERIAL AND METHODS

2.1 IN VITRO EXPERIMENTS

2.1.1 Full length recombinant mouse PrP (Mo-recPrP) cloning, expression and purification.

DNA primers (forward 5'-CTGTCTAGAATGAAAAAGCGGCCAAAGCCTGG-3' and reverse 5'-TTAGGATCTTCTCCCGTCGTAATA-3') were synthesized and used to amplify by PCR the mouse *prp* gene 23-230 from C57 mouse genomic DNA extracted from tails. The products were cloned into pET303/CT-His (Invitrogen®) plasmid and expressed in E. coli. For expression, freshly transformed cells were grown in 5 ml of Terrific Broth medium supplemented with carbenicillin (100 ug/ml) at 37°C for 6 h. The starter culture was then diluted into 50 ml of the same medium and grown for another 6 h. This culture was finally diluted into 750 ml of the same medium and grown until it reached 0.7 OD. One millimolar IPTG (isopropyl □-D-thiogalactopyranoside) was then added, and the cells were induced for 5 h. The culture was harvested by centrifugation and stored at -80°C. For purification, cell pellets were thawed and resuspended in buffer A (50mM Tris-HCl, pH 8.0, 1mM EDTA, and 100mM NaCl). Cells were lysed by adding 0.5 mg/ml lysozyme and subsequently sonicated. The released inclusion bodies were pelleted by centrifugation at 22,000 g and then washed twice with buffer A supplemented with 0.05% (v/v) Triton X-100. The inclusion bodies containing recPrP were solubilized for 2 h with buffer B (10mM Tris-HCl, 100 mM Na2HPO4, pH 8.0, 100 mM NaCl, 10 mM -

mercaptoethanol, 6 M GdnCl) and then purified by using standard immobilized metal affinity chromatography procedure. Briefly, the sample was bound to Ni Sepharose 6 Fast Flow resin (GE Healthcare) in batch mode for 1 h at room temperature and then washed with buffer B. RecPrP was on-column refolded for 6 h and eluted with buffer B supplemented with 500 mM imidazole and without GdnCl. The main peak was collected and quickly filtered to remove aggregates. The sample was buffer exchanged using Zeba desalting columns (Pierce®), further concentrated to ~0.5 mg/ml, and flash-frozen at -80°C. Protease inhibitors (Complete® protease inhibitor mixture from Roche) were used throughout the purification to minimize degradation. The protein was confirmed to be monomeric and folded by SDS-PAGE, Western blotting, and circular dichroism

2.1.2 Aggregation assays in the presence of salts. All reactions were carried out in 0.5 mL Lo-Bind Eppendorf tubes (protease/nuclease free grade and further autoclaved). All reagents were of highest available quality and protease-free grade when available. Protease-free nanopure water was used to prepare all master solutions and reactions. Thawing of recPrP was followed by filtration through 100 kDa-cutoff Microcon tubes (Millipore) to remove possible aggregates formed upon thawing. Protein concentration was re-estimated upon filtration by spectrophotometry. RecPrP (0.1 mg/mL final concentration) was mixed with 40 mM Hepes pH 7.2 and different concentrations of salts in 100 uL final volume reactions. pH was re-adjusted upon salt addition. Aggregation experiments were conducted using a protocol adapted from previous reports [44]. Unless specified, reactions were placed in an Eppendorf Thermomixer for 24 hrs at 37°C with cycles of 1 minute agitation at 1500 rpm and 1 minute incubation. Samples were then treated with Proteinase K (PK) at a 1/10 molar ratio (PK/recPrP) for 1 h at 37°C (water bath) unless specified differently. Analysis of digestion assays was performed by SDS-PAGE followed by Western blotting and silver staining. Antibodies 6D11 and M-20 were used for the analysis.

2.1.3 Aggregation assays in the presence of co-factors. Reagents and tubes were of the same grade and quality as described above. Thawing of Mo-recPrP was followed by filtration through

100 kDa-cutoff Microcon tubes (Millipore) to remove possible aggregates formed upon thawing. Protein concentration was re-estimated upon filtration by spectrophotometry. Mo-recPrP (0.1 mg/mL final concentration) was mixed with phosphate buffer saline (PBS), 0.1% triton and 0.1% SDS in a 100 uL total volume reaction according to previous reports[38, 44]. Aggregation experiments were conducted using a protocol adapted from the same reports: unless specified, reactions were placed in an Eppendorf® Thermomixer for 24 hrs-round at 50°C with cycles of 1 minute agitation at 1500 rpm and 1 minute incubation. In serial passages experiments, 10 uL of the first round were mixed with 90 ul of a fresh mixture and submitted to a new 24 hrs-round. Samples were then treated with Proteinase K (PK) at a 1/40 molar ratio (PK/PrP) for 1 hrs at 37°C (water bath) unless differently specified. Analysis of digestion assays was performed by SDS-PAGE followed by Western blotting. Antibodies 6D11 and M-20 were used for the analysis.

2.1.4 Effect of co-factors on PK-resistance after aggregation. The aggregates formed after serial amplification rounds as described above were centrifuged at 18000 x g for 30 min at room temperature and then resuspended in an equivalent volume of PBS. This washing step was repeated 4-5 times. The pellet obtained in the final washing step was resuspended in PBS supplemented with different co-factors at different concentrations as specified in the figures. The samples were then incubated at 37°C for 3 hrs and submitted to PK digestion assays (1 hrs incubation at 37°C). The analysis of the digestion products was performed by SDS-PAGE followed by Western blotting.

2.1.5 Thioflavin T binding assay. Highly pure thioflavin-T (Th-T) dye stock solution was added directly to reactions to a final concentration of 10 uM in black-walled 96-well plates. Fluorescence measurements of the samples were taken using a Microplate Reader Accessory adapted to a Hitachi Fluorescence Spectrophotometer F-7000, using an excitation wavelength of 435 nm and recording in the emission range between 400 and 600 nm. A scan speed of 240 nm/min was used as standard for all readings. To reduce interference noise from excitation light, a 475 nm emission cutoff filter was used.

2.1.6 Fourier-Transform Infrared spectroscopy (FTIR). FTIR experiments were conducted in an FT/IR-4100 spectrometer from JASCO. PrP^{Sc} used in this work was obtained from RML-infected mouse brains and was purified as follows: 10% brain homogenates containing 10% sarkosyl were loaded onto a 20% sucrose cushion and centrifuged at 150,000 x g for 3 hrs. The pellet was resuspended in Z3-14 zwitterion detergent, then loaded onto 20% sucrose cushion and centrifuged at 150,000 x g for 3 hrs. This step was repeated twice. Pellet was finally resuspended in 1X PBS buffer and washed twice using the same 20% sucrose cushion. The PBS-resuspended pellet was shown to be highly pure by silver staining after electrophoresis (data not shown). PrP^{Sc} concentration was estimated by software-based signal intensities calculation upon Western Blotting based on known concentrations of soluble recPrP. Before measurements, PrP aggregates were concentrated by ultracentrifugation at 150,000 x g for 1 h at 4C. Protein slurry was then added on top of a diamond PRO450-S Attenuated Total Reflectance unit from JASCO adapted to the FT/IR-4100 system. System parameters included 4.0 cm-1 resolution and an accumulation of 64 scans per sample. Data fitting and secondary structure calculations of samples were analyzed by multi-component analysis through the Secondary Structure Estimation (SSE) software from JASCO. Each sample measurement was optimized until the corrected experimental data and the fitting curve gave minimum absorbance differences.

2.1.7 Negative staining-Transmission Electron Microscopy (TEM). RecPrP aggregates were directly loaded on grids. Previously to TEM analysis, PrP^{Sc} was partially purified using 10% brain homogenates containing 10% (v/v) sarkosyl from RML-infected mice. Briefly, brain homogenates were loaded onto a 20% (g/v) sucrose cushion and centrifuged at 150,000 x g for 3 hrs. The pellet was resuspended in Z3-14 zwitterion detergent, then loaded onto 20% (g/v) sucrose cushion and centrifuged at 150,000 x g for 3 hrs. This step was repeated twice. Pellet was finally resuspended in 1X PBS buffer and washed twice using the same 20% (g/v) sucrose cushion. The PBS-resuspended pellet was shown to be highly pure by silver staining after electrophoresis. Protein aggregates were directly put on FORMVAR–coated copper grids, air-dried for 5 minutes followed by filter-paper-drying of reaction excess. Grids with samples were

negatively stained with 1% uranyl acetate for 1 min, wick off excess and dry for another 5 min at 70C. Imaging was performed on a JEOL 1200 transmission electron microscope at 60 kV and captured by 1kX1k Gatan BioScan 792 CCD camera.

2.1.8 Cell Viability Assay. N2A cells were cultured in DMEM supplemented with 10% fetal calf serum and antibiotics (10,000 U/ml Penicillin, 10 mg/ml streptomycin), at 37°C and 5% CO_2. For cell viability analysis, cells were grown in collagen IV coated 96-well plates for 48 hrs in cell culture medium containing 1% serum before addition of recPrP aggregates and control reactions. Cell viability was quantified using 3-(4,5-dimethylthazol-2-yl)-5-3-carboxymethoxy-phenyl)-2-(4-sulfophenyl)-2H-tetrazolium (MTS) and phenazine methosulfate (PMS) according to the recommendations of the supplier (Roche).

2.2 IN VIVO EXPERIMENTS

2.2.1 Infectivity studies of recPrP on bioassays. All aggregated forms of recombinant PrP were tested for their infectious properties in wilt-type mice. Five-microlitter samples containing approximately 5-10 ug of protein were inoculated intra-cerebrally into 1-month old female mice by stereotaxic injection into the hippocampal area. Ten animals were used per specific sample.

CHAPTER 3

CONVERSION AND MISFOLDING OF PRION PROTEIN IN THE ABSENCE OF ORGANIC CO-FACTORS

3.1 ABSTRACT

Prions are self-propagating proteins involved in transmissible spongiform encephalopaties in mammals. An aberrant conformation with amyloid-like features of a cell surface protein, termed prion protein (PrP), is thought to be the essential component of the infectious particle, though accessory co-factor molecules such as lipids and nucleotides may be involved. The cellular co-factors and environmental conditions implicated in PrP misfolding are not completely understood. To address this issue, several studies has been done inducing misfolding of recombinant PrP (recPrP) into classical amyloid structures using partially denaturing conditions. In this work, I found that misfolding of recPrP into PrP^{Sc}-like aggregates can be induced by simply incubating the protein in the presence of kosmotropic salts at

concentrations that are known to retain or increase the stability of the protein. I used a simple experimental reaction (protein, buffer and salts) submitted to agitation/incubation cycles at physiological temperature and pH. The formation of protease resistant-recPrP was time and salt-concentration dependent and required the presence of kosmotropic anions such as F^- or SO_4^{-2}. The molecular weights of the protease resistant recPrP fragments are reminiscent of those found in degradation assays of bona fide PrP^{Sc}. The aggregates also exhibited amyloid-like features such as high beta-sheet content and thioflavin-T positive signal. The formation of recPrP aggregates with PrP^{Sc} biochemical features under conditions closer to physiological in the absence of organic co-factor molecules provide a simple setup that may prove helpful to understand the molecular mechanism of PrP misfolding.

3.2 INTRODUCTION

Transmissible spongiphorm encephalopaties (TSEs) are fatal and infectious neurological maladies in mammals caused by prions. The infectious agent is primarily composed of an aberrantly folded glycosylated protein termed prion protein (PrP), which is mainly expressed in the brain [5, 6]. Misfolded PrP in its prion state (PrP^{Sc}) acquire self-propagation features to induce the transformation of the normal PrP conformation (PrP^{C}) into the infectious form [16]. In vitro experiments using brain extracts from infected and uninfected animals have shown that it is possible to harvest prions in the test tube and recapitulate most of the biochemical and pathological events by the so-called PMCA (protein misfolding cyclic amplification) approach [33, 34]. Despite these great advances, understanding the molecular details of the protein conversion mechanism requires experimental setups relying on pure and defined components mimicking most of the features associated to prion formation. Experiments using exclusively recombinant PrP (recPrP) have so far failed to show infectivity in wild-type animals in a first passage [35, 36]. However, highly infectious synthetic prions have been reported using mixtures of recPrP, lipids and mouse-extracted RNA molecules submitted to PMCA [37]. RecPrP aggregates with highly heterogeneous infectivity were also achieved using modified PMCA experiments in reactions

containing recPrP and mixtures of detergents (SDS and triton) [38, 39]. The lack of transmissibility of exclusively protein-only inoculates suggests that accessory co-factor molecules may be essential for prion infectivity in mammals [40, 41, 45].

Experimental approaches aimed to induce the conversion of recPrP into amyloid-like aggregates with some of the features associated to PrP^{Sc} have classically relied on the use of chemical and/or physical agents promoting partial or total protein denaturation such as guanidine hydrochloride, urea, SDS, temperature, pH, etc. [38, 46-53]. Most of these protocols yield recPrP aggregates resembling typical amyloid fibrils. This is in agreement with the current hypothesis that most, if not all, proteins have intrinsically the capability to be converted into amyloids [12]. Despite the fact that PrP^{Sc} isolates also show some amyloid-like features, it is unclear whether the formation of large amyloid aggregates is necessary for infectivity. Indeed, PrP^{Sc} typically appears as amorphous aggregates with little presence of defined fibrils under the microscope [54, 55]. RecPrP has been converted into PrP^{Sc}-like aggregates when combined with lipids under physiological conditions and in the absence of denaturants [56]. Interestingly, as mentioned above, these same aggregates were later shown to be infectious in wild-type mice when RNA molecules were added to the mixture that was then subjected to PMCA cycles [37].

Salts have been previously used as a more physiological way of inducing protein misfolding and formation of amyloids [57-60]. It has been previously demonstrated that recPrP show a dual behavior in the presence of stabilizing salts, which is characterized by an initial destabilization at low concentrations followed by stabilizing effects at high concentrations according to the Hofmeister series [61]. Sodium chloride can stimulate formation of recPrP amyloid in a concentration dependent manner under non-physiological conditions including very low pH and high temperatures [57]. Here, I tested the effect of kosmotropic/stabilizing salts on the misfolding pathway of full-length recPrP using strictly physiological temperature and pH. The results show that kosmotropic anions specifically promote formation of PrP^{Sc}-like aggregates in reactions containing only protein as the main organic molecule.

3.3 RESULTS

3.3.1. Kosmotropic salts induce formation of protease-resistant fragments of full length recPrP. Prions composed of brain-derived PrP^{Sc} are known to be partially resistant to degradation by proteases [5]. I incubated recPrP in the presence of various salts to test the formation of protease-resistant material. I focused The analysis on the kosmotropic/stabilizing side of the Hofmeister series. Sodium fluoride (NaF) is a known kosmotropic agent that promotes stabilization of structured states of most proteins, including recPrP at high salt concentrations [61]. Incubation of recPrP at different concentrations of NaF using agitation/incubation cycles (see Experimental Procedures) led to the formation of a 17 kDa protease-resistant fragment ($recPrP^{res}$) as shown by Western Blotting analysis (Fig. 1A). The salt concentration at which $recPrP^{res}$ was first detected was around 400 mM. At lower concentrations I did not observe any protease-resistant material. The main degradation fragment exhibited a 17 kDa molecular weight, which is in agreement with the sizes reported for unglycosylated GPI-less PrP^{Sc} [54]. I also noticed that at high concentrations of salt, the signal of undigested recPrP also increased, which may be indicative of salting-out effects occurring during the reactions.

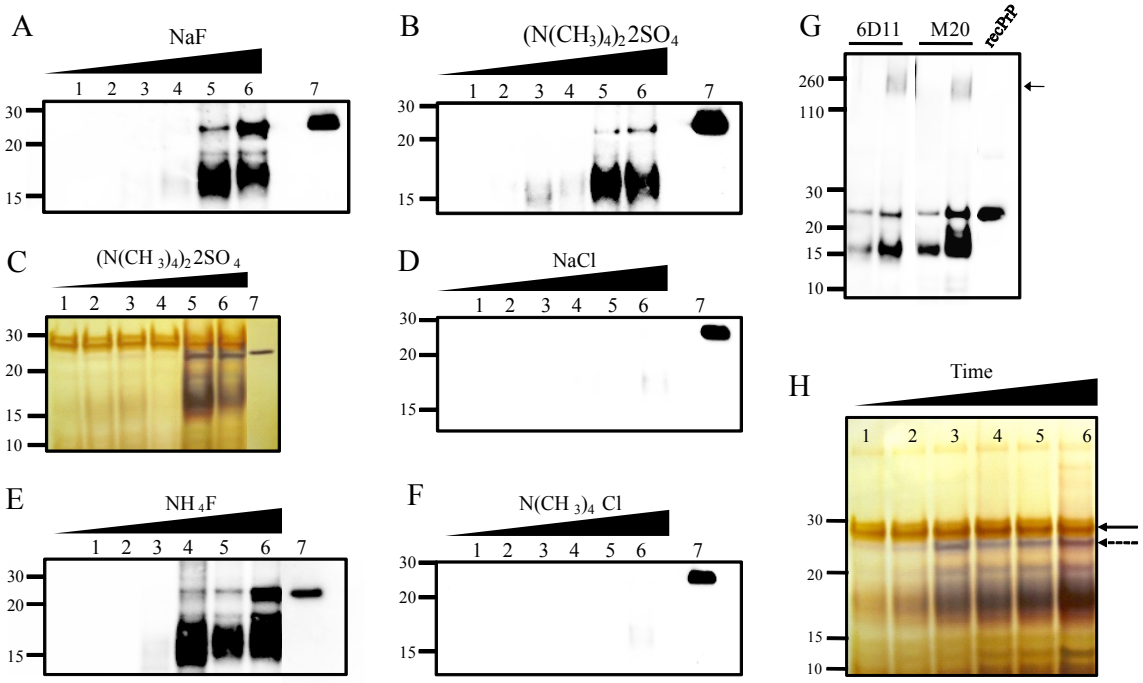

Figure 3.1: *Formation of protease-resistance recPrP (recPrP^{res}). A-F*. RecPrP was incubated with different concentrations of NaF (*A)*, $(N(CH_3)_4)_2SO_4$ (*B,C*), NaCl (*D*), NH_4F (*E*) and $N(CH_3)_4Cl$ (*F*) as described in materials and methods, followed by Western Blotting (*A,B, D-F*) or silver staining (*C*). Salts concentrations (mM) for the reactions were 0, 100, 200, 300, 400 and 500 for lanes 1, 2, 3, 4, 5 and 6, respectively. Undigested recPrP is shown on lane 7 for each figure. *G*: Antibody mapping analysis of protease resistance fragments was performed using a 400 mM NH_4F-based reaction incubated for 24 hrs. Duplicated samples at two different dilutions (1/2 and 1/1 per left and right lane, respectively) were western-blotted using monoclonal antibodies 6D11 and M-20. The arrow indicates the presence of oligomeric species. *H*: Time-course experiments. RecPrP was aggregated in 400 mM NH_4F for different times: 0 hrs (lane 1), 3 hrs (lane 2), 10 hrs (lane 3), 24 hrs (lane 4), 72 hrs (lane 5) and 144 hrs (lane 6) and the recPrP^{res} product was analyzed by silver staining. PK signal is highlighted by the solid arrow. The undigested recPrP signal is indicated by the dashed arrow. In all panels, samples were digested using PK at 1/10 PK/recPrP ratio for 1 hrs at 37°C and then subjected to either western blot or silver staining. Molecular weights markers (kDa) are shown on the left side of each panel.

In order to analyze whether the observed effect caused by NaF was salt-specific, I studied the effects of other known kosmotropic/stabilizing salts on the misfolding of recPrP. For this I used another kosmotropic salt carrying both a highly stabilizing anion (SO_4^{-2}) and cation (($N(CH_3)_4^+$). Similar results were observed in terms of induction of salt concentration-dependent protease-resistant recPrP (Fig. 1B). To study whether other protease-resistant aggregates not recognized by the antibody used were being produced, I stained the gel using silver nitrate. The results show that the 17 kDa is the most abundant protease resistant fragment with only very faint signal associated to lower molecular weight fragments (Fig. 1C). To test whether the effect observed was specifically due to kosmotropic/stabilizing salts, I studied the effect of sodium chloride (NaCl), a rather neutral salt in terms of protein stability. Surprisingly, the formation of protease-resistant fragments was virtually eliminated compared to those formed under the presence of kosmotropic salts (Fig. 1D), suggesting that the formation of protease-resistant fragments described above required kosmotropic salts.

I then asked whether this kosmotropic-dependent effect was dependent on the cation or anion. For this purpose I used a salt that retains the stabilizing anion (F^-) and incorporates a more stabilizing cation (NH_4^+). The effect was similar as those observed with NaF, i.e. partial protease resistance which was concentration-dependent with similar molecular weights of the main proteolytic fragments (Fig. 1E). However I noticed an increase in the signal of the protease-resistant fragments compared to those formed in the presence of NaF (Fig. 1A). In addition, the protease-resistant fragments appeared at lower salt concentrations compared to NaF. Next, I tested $(N(CH_3)_4)Cl$, a salt carrying a highly kosmotropic cation and Cl^- as a neutral-to-destabilizing anion. Notably, as it happened with NaCl, I did not observe the formation of any protease-resistant fragment at any molecular weight size range (Fig. 1F), suggesting that a stabilizing anion is key to promote the formation of protease-resistant fragments. In order to rule out an adverse effect of the salts in the proteolytic activity of PK, I used BSA as a control and

confirmed that PK retains its proteolytic activity even in the presence of relatively high concentrations of kosmotropic salts (data not shown).

3.3.2 Antibody mapping of salt-induced recPrP^{res}. PrP^{Sc} degradation occurs at the N-terminal region of PrP, implying that the protease-resistant material that retains infectivity properties is a C-terminal truncated portion of PrP [62-64]. In order to map the topology of the protease-resistant bands observed after incubation with kosmotropic salts, I used two different antibodies. mAB 6D11 is known to target a region between 93-109 within PrP of different species, including mouse. I also used the polyclonal antibody M-20 that recognizes an epitope near the C-terminus of PrP. All the protease-resistant fragments gave positive signal with both antibodies, suggesting that the products exhibit a similar mapping profile to that of PrP^{Sc} (Fig. 1G).

3.3.3 Time-dependent formation of recPrP^{res}. A time-course experiment was performed in order to evaluate the progress of the reaction over time. I chose NH_4F as the kosmotropic salt and followed the reaction for several days by silver staining analysis in order to provide a full spectrum of protease-resistant fragments. A master solution including recPrP and NH_4F was divided into 6 time-points reactions in order to decrease error. The formation of protease-resistant fragments slowly increased and reached saturation after 4-6 days (Fig. 1H). I also noticed that the intensity of the lower molecular weight protease-resistant species increased in time in a similar way as those of higher sizes. Moreover, the signal of the band associated to undigested full length recPrP also increased with a similar pattern. However, after several hours of reaction, this signal remained steady, while the protease-resistant digested products kept increasing, suggesting a more specific effect of the salt on the formation of the PrP^{Sc}-like protease-resistant species.

3.3.4 Structural characterization of recPrP^{res} aggregates. To study whether the PK-resistant aggregates had amyloid-like characteristics I tested their binding to Th-T, a well-known amyloid-binding die [49, 65]. After 24 hrs of incubation in presence of NH_4F, the aggregates gave a Th-T positive signal which was approximately 14 times higher than the signal at time 0, suggesting the formation of amyloid-like aggregates (Fig 2A). In control experiments, I observed

that high concentrations of NH_4F had minimal effect on the bare Th-T signal (data not shown). To study whether fibril formation followed a seeding-dependent kinetic typical of amyloids I studied the Th-T signal as a function of time. The formation of Th-T positive aggregates exhibited a classical sigmoideal behavior with a lag-phase of around 10 hrs, followed by a exponential face, reaching a maximum at around 28 hrs (Fig. 2B) and then decay of the signal, probably due to formation of Th-T-inaccessible clumps of aggregates.

To study the ultrastructural features of salt-induced $recPrP^{res}$ aggregates, samples were analyzed by TEM. The results showed that the aggregates formed by recPrP in the presence of NH_4F were similar to those present in highly purified PrP^{Sc} obtained from the brain of prion infected animals (Fig. 2C). In both samples, I observed rod-like aggregates which formed large clumps of aggregates. Little or no classical amyloid fibrils were seen in any of the preparations.

To further study the structural features of these aggregates I analyzed salt-induced $recPrP^{res}$ by FTIR spectroscopy and compared it to soluble recPrP and purified PrP^{Sc}. Both $recPrP^{res}$ aggregates and PrP^{Sc} showed a main absorbance peak at around 1639 cm^{-1} which is indicative of predominant beta-sheet secondary structure, while soluble recPrP exhibited high alpha-helical content, peaking at around 1658 cm^{-1} (Fig. 3A). A deconvolution analysis showed typical secondary structure contents of alpha-helical proteins for soluble recPrP, with a large fraction of random structure, which is most likely associated with the long natively-unfolded PrP N-termini region (Fig. 3B). Conversely both $recPrP^{res}$ and PrP^{Sc} exhibited mainly beta-sheet structure with some residual alpha helical content.

3.3.5 Citotoxicity of salt-induced $recPrP^{res}$. I next sought to test whether the protease-resistant fragments generated in the presence of salts acquire toxic features against neuroblastoma cells. Initially I attempted performing the experiments adding directly the recPrP incubated with salts onto the cells. However, NH_4F *per se* was highly toxic to cells (data not shown). Thus, I first removed the salt by extensive dialysis before adding the proteins to the cell cultures. Under these conditions I observed high levels of toxicity of $recPrP^{res}$ as measured by the MTT cell viability assay (Fig. 4). The citotoxic activity occurred at very low concentrations of $recPrP^{res}$ comparable

to those produced by PrP^{Sc} purified from the brain of prion infected animals. These concentrations are 1000-times lower than those used with small PrP fragments polymerized into amyloid fibrils[66, 67]. As expected, soluble recPrP and the dialysis buffer gave a near-to-zero toxicity (Fig. 4).

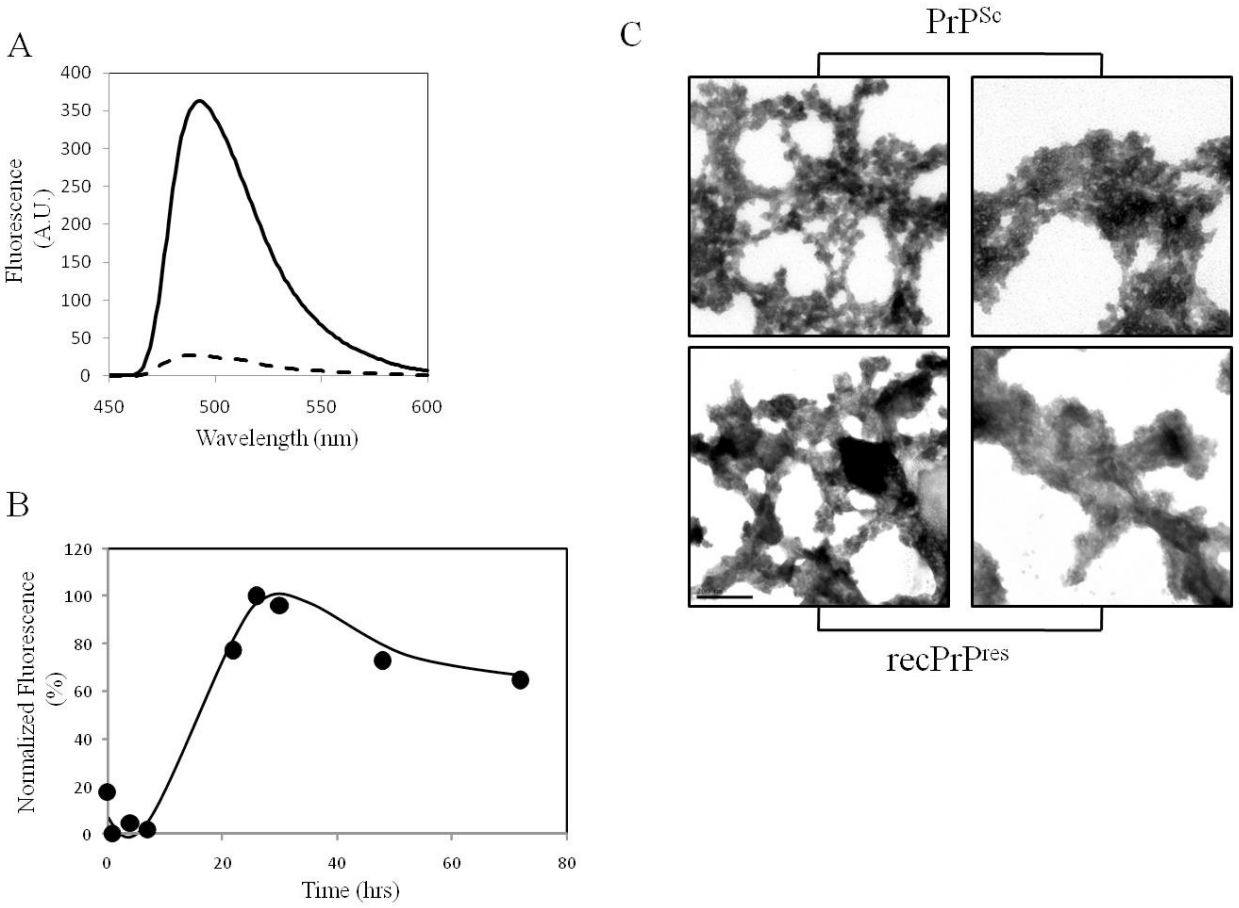

Figure 3.2*: RecPrP^{res} forms aggregates with some but not all characteristics of amyloid fibrils*. *A:* RecPrP was incubated for 0 hrs (dashed line) or 22 hrs (solid line) with 400 mM NH_4F and then fluorescence emission spectra of samples in the presence of 10 uM Th-T was recorded. An emission maximum was obtained at 491 nm when excited at 435 nm, typical of amyloid-like aggregates. *B*: the kinetic of recPrP aggregation was evaluated by incubating the protein in the

presence of 400 mM NH_4F for different times. At indicated time points, Th-T emission was measured at 491nm with excitation set at 435nm. *C*: To study the morphology of the recPrP aggregates, samples were loaded onto EM grids, stained with silver nitrate and visualized under transmission electron microscopy (TEM). Two representative images at different magnification are shown for both PrP^{Sc} and $recPrP^{res}$ aggregates. The bar corresponds to 200nm.

A

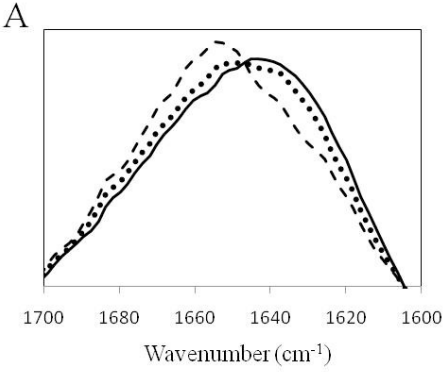

B

	Alpha helix (%)	Beta sheet (%)	Beta turn (%)	Random (%)
recPrP (soluble)	28	20	25	27
recPrP aggregates	9	47	20	24
PrP^{Sc} (RML)	13	34	25	28

Figure 3.3: *Secondary structure of $recPrP^{res}$ aggregates*. *A*: Buffer and baseline-corrected FTIR spectra of salt-induced $recPrP^{res}$ aggregates (solid line) compared to those of soluble recPrP (dashed line) and PrP^{Sc} purified from the brain of mouse infected with RML prions (dotted line). FTIR spectra were obtained using the conditions described in Materials and Methods. *B*: The percentage of different secondary structure motifs on $recPrP^{res}$ aggregates, soluble recPrP and purified PrP^{Sc} was estimated by deconvolution of spectra using the Secondary Structure Estimation (SSE) software from JASCO.

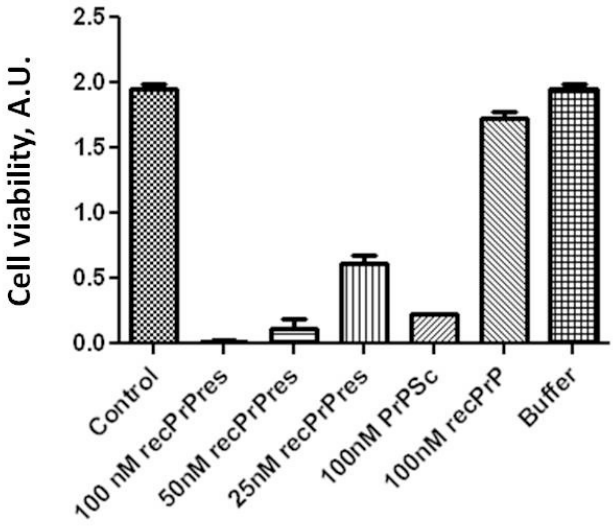

Figure 3.4: *RecPrP^{res} aggregates are similarly neurotoxic as PrP^{Sc}*. RecPrP^{res} aggregates were produced by incubation for 24 hrs with 400mM NH_4F. 100, 50 and 25 nM of dialyzed recPrP^{res} aggregates were added to the medium of $1x10^5$ N2A neuroblastoma cells and cell viability was measured after 24 hrs of incubation using the MTT assay. As a negative control, the same volume of PBS was added to the well (control). Purified RML-PrP^{Sc} (PrP^{Sc}), soluble recPrP (recPrP) and the reaction buffer without protein (buffer) were also assayed as controls. All experiments were done in triplicate and the values correspond to the average ± standard error. The reduction of cell viability produced by addition of recPrP^{res} or PrP^{Sc} was highly significantly ($P<0.001$) different from soluble recPrP and the buffer control, as determined by student t-test.

3.3.6 Infectivity of aggregated recPrP. Aggregated recPrP produced by incubating PrP for 24 hr in the presence of 400 mM NH_4F was intra-cerebrally inoculated into wilt-type mice to test the self-propagation ability of salt-induced misfolded PrP *in vivo*. This experiment is currently ongoing.

3.4 DISCUSSION

PrP misfolding is a central event in the pathogenesis of prion diseases. The mechanism responsible for the PrP^{C} to PrP^{Sc} conversion and the potential role of accessory molecules in this process are not completely understood [41, 55]. Several *in vitro* models have been proposed to study the mechanism of prion conversion. Among them extensive studies have been done using recPrP forced to aggregate into amyloid fibrils by using partially denaturing conditions, including chemical (guanidine hydrochloride, urea, SDS, etc.) and/or physical denaturants (temperature, pH, pressure, etc.) [38, 46-53]. In some of these studies recPrP aggregates displayed various biochemical and even infectious properties of PrP^{Sc} [35, 39, 49]. All of these experimental approaches rely on the assumption that partially unfolding states of the protein are directly involved in the amyloid formation pathway [12, 68]. In this work, I aimed to test whether recPrP can be folded into a PrP^{Sc}-like conformation by more physiological conditions, and in the absence of any organic molecule, using exclusively stabilizing salts.

The results indicate that protease-resistance recPrP aggregates with some of the biochemical features typical of PrP^{Sc} are readily formed in the presence of stabilizing, kosmotropic salts. The protease resistance fragments exhibited an approximated size of 17 kDa, which is in agreement with sizes reported for PrP27-30 (subtracting the weights associated to GPI anchor and glycans) [5, 54]. Smaller fragments were also observed albeit at much lower ratios. Although the salts used in this study are not considered denaturing agents, they may have some impact on the activity of the protease used in The studies. To rule out any significant effect of the salt on the protease activity, I did a control digestion assay of BSA in the presence of PK. I observed that PK degradation ability was not affected by the salt concentrations used in the assay (data not shown). This is not surprising considering that PK is completely active at high concentrations of NaCl [69]. Additional evidence to rule out an effect of the salt in protease activity comes from the time-course experiments. As showed in figure 1H at short times of incubation with salt only a faint signal of protease-resistant recPrP is observed, despite the fact that the PK digestion conditions were the same as those in which a high quantity of $recPrP^{res}$ was observed.

The recPrP^{res} aggregates exhibited classical features associated to amyloids such as an increase in Th-T fluorescence emission, sigmoideal time-dependent aggregation mechanism and changes in secondary structure leading to higher contents of beta-sheet. However, I was not able to observe formation of typically well-defined amyloid fibers by TEM analysis. Classical amyloid fibrils are typically formed by using partially denaturing conditions, as it has been shown for recPrP in various reports [36, 46, 49, 50, 70, 71]. On the other hand, bona fide PrP^{Sc} isolated from the brains of prion infected wild-type animals usually exhibits relatively low content of amyloid fibrils (Fig. 2C) [54, 55]. Interestingly, the morphology of the aggregates consisting of clumps of rod-like structures was very similar between PrP^{Sc} and salt-induced recPrP^{res} (Fig. 2C). It is possible that kosmotropes-induced aggregates follow a different aggregation pathway than those formed under partially denaturant conditions, by for instance retaining some native like structure. Amyloids generated under non-denaturing conditions have been previously shown to exhibit such features [68]. In this study, the aggregates were shown to primarily contain beta-sheet structures, although some alpha-helix signal remained.

The mechanism by which kosmotropic salts induce PrP^{Sc}-like properties in recPrP is not known, but may involve a specific interaction with the protein promoting conformational changes (Fig. 5). Salts have been previously shown to be required by PrP^{Sc} in order to exhibit full protease resistance features [69]. One potential scenario for the PrP PK-resistance observed upon incubation with kosmotropic anions may be simply due to electrostatic binding of ions to the highly basic N-terminal region blocking the access to cleavage sites by the protease (Fig. 5A). However I consider this scenario unlikely since chloride ion did not exert a significant effect (Fig. 1D). Moreover, positive charges are spread all over the N-terminal domain, which should cause an overall, unspecific protection against degradation. I also rule out a high specificity for the kosmotropic anion due to the high salts concentrations required to observe the protease-resistant bands and the fact that different kosmotropic anions produce a similar result. Accordingly, stabilizing salts may promote PrP misfolding by increasing the local concentration of the protein through salting-out mechanisms (Fig. 5B). Under this scenario, folding

intermediates or even PrP^{Sc}-like particles originally present at very low concentrations would increase their effective concentration, accelerating the nucleation and seeding processes. However, salting-out by itself may not be the only mechanism involved, because kosmotropic cations were not able to promote protease-resistance (Fig. 1F). Soluble recPrP is known to be thermodynamically stabilized at high concentrations of kosmotropic anions such as fluoride and sulfate, whereas chloride induces a rather destabilizing effect [61]. In this work, these two kosmotropic anions strongly stimulated formation of protease-resistant aggregates, whereas chloride, even when bound to a highly stabilizing cation, did not have a detectable effect. Sulfate and phosphate anions decorating the surface of certain macromolecules such as heparan-sulfate and polynucleotides have been proposed to play a role in PrP conversion [55, 72-74]. Interestingly, these macromolecules have also been proposed to serve as scaffolds that concentrate PrP molecules on its surface in addition to providing structure-compatible negatively charged groups, thereby acting as a potential catalyst for PrP^{Sc} formation [73, 75-78]. This work is consistent with those reports, suggesting that increased local concentrations may be critical for the conversion process. In addition, the acquisition of protease-resistance in part of the natively unfolded N-terminal domain may be a manifestation of disorder-to-order structural transitions within the region that are induced and/or stabilized by the stabilizing anions (Fig. 5C). In the presence of more kaotropic/denaturing anions as used in most conversion protocols for amyloid formation, this natively unfolded region would be kept from acquiring any significant structure.

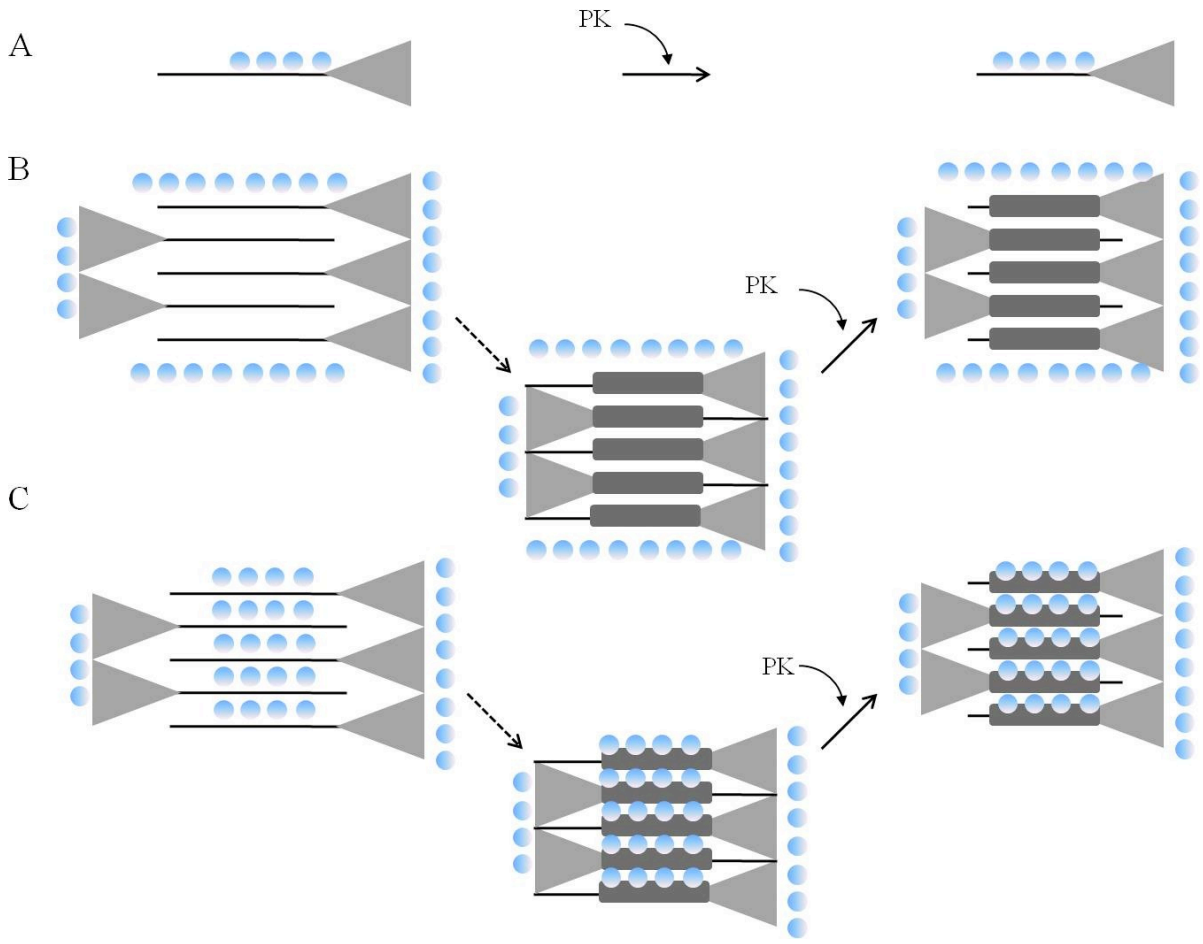

Figure 3.5: *Potential mechanisms for recPrP aggregation induced by kosmotropic salts*. The soluble monomeric recPrP is represented as a two-domain protein, C-terminal globular domain (triangle) containing a large proportion of alpha-helical structure and the natively-unfolded N-terminal domain (solid line). RecPrP with the dark gray horizontal rectangle (representing beta-sheet secondary structure) corresponds to the misfolded protein. The kosmotropic anions are represented by the blue circles. The dotted arrows indicate a misfolding process, while the solid arrows represent the protease digestion reaction (PK). Three putative models to explain the effect of the salt on inducing the formation of $recPrP^{res}$ are proposed. *A:* Binding of kosmotropic anions may occlude specific cleavage sites within the N-terminal domain. This model could explain the protease-resistance, but does not account for the structural changes induced by salt. *B*: A salting-out-like mechanism locally increases PrP concentration in a native-like conformation, followed

by either an induction or acceleration of intermolecular beta-sheet formation leading to PrP^{Sc}-like aggregates. *C*: A combined effect of high concentrations of kosmotropic anions that partially salt-out recPrP in a close-to-native fold from the bulk solution, along with specific anion binding and further stabilization of part of the N-terminal domain induce a protease-resistant recPrP conformation with PrP^{Sc} features.

These studies demonstrate that recPrP aggregates exhibiting PrP^{Sc}-like biochemical properties can be readily formed using stabilizing salts. Synthetic infectious prions have been achieved using recPrP, lipids and mouse-derived RNA molecules (7). Highly variable infectivity was also reported using recPrP in a mixture of detergents and saline buffer [38, 44]. The formation of prions made out of strictly protein in buffer without organic additives has not been achieved so far. Here I present a system in which recPrP misfolding with features associated to PrP^{Sc} can be induced only by varying the concentration of kosmotropic anions in a close-to-physiological experimental setup. Infectivity studies with these samples are currently ongoing. If these studies show the generation of infectivity, salts may represent the simplest "co-factor" molecule

CHAPTER 4

CONVERSION AND MISFOLDING OF PRION PROTEIN IN THE PRESENCE OF ORGANIC CO-FACTORS

4.1 ABSTRACT

Prion diseases are infectious neurological maladies transmitted by an unconventional "*proteinaceous*" agent. The prion protein (PrP) is thought to be an essential structural component of the infectious unit, though the involvement of other accessory molecules is still not clear. The details about the molecular nature of prions are not known as well as the precise mechanism of prion propagation. One of the main biochemical hallmarks of prion is their high resistance to protease degradation. In order to obtain insights about the potential role of non-PrP molecules on the molecular properties of prions, I studied the in vitro effect of different co-factors molecules on the acquisition of protease-resistance. I found that the extent of resistance to protease-degradation of PrP seems to be mediated by electrostatic forces as well as by the nature of the accessory molecule. Moreover, the effect of all molecules studied was highly reversible, suggesting that co-factors modulate the protease-resistance feature of prions.

4.2 INTRODUCTION

The prion hypothesis states that the infectious agent underlying prion diseases is a misfolded form of PrP[4]. This abnormally folded conformation is believed to provide PrP with self-propagation capabilities that will enable it to recruit normally folded PrP inside the brain into the infectious form (PrP^{Sc}), which will bring as a consequence neuronal degeneration and

finally death[4, 79, 80]. PrP is known to be an essential component of the prion particles, as has been experimentally demonstrated many times[5-7, 25, 81, 82]. The absolute resistance of PrP knock-out mice to prion infection as well as the PrP-dependent infectivity of protein extractions from prion-infected brains has settled most doubts about the involvement of PrP in prion diseases[6, 7]. However, the efforts to prepare infectious particles using only PrP have so far failed[35, 36]. Moreover, the involvement of accessory molecules as essential components of the infectious particle has recently gained great interest[73, 83].

A key event during PrP misfolding is the acquisition of partial resistance to protease degradation[5]. Some other prion and amyloids have also exhibited partial protease-resistance, though in those cases the extent of resistance is much less compared to mammalian prions[84-86]. The region within PrP^{Sc} that acquires protease-resistance is a C-terminal fragment spanning from residues ~90 to 230[87], as opposed to all other prions and amyloids in which the whole protein becomes resistant to degradation. Although the structural details accounting for protease-resistance have not been elucidated, it is believed that at least in part, the formation of stable aggregates with highly ordered stacks of b-sheets causes stabilization of the prion conformation and occludes cleavage sites[5, 88]. The fact that PrP^{Sc} is not entirely protease-resistant suggests that only part of the protein acquires a prion-compatible misfold, with sizes in the range between 15 and 20 kDa[5]. Moreover, in vivo experiments using transgenic mice expressing truncated PrPs demonstrated that the minimal and necessary fragment required for prion infection starts from around residue 90[89, 90].

Infectious prions using pure, defined components were first achieved using reactions containing brain-derived PrP, co-purifying lipids and RNA molecules[73]. PrP^{Sc}-like species were formed spontaneously after submitting the mixture to several cyclic rounds of amplification through PMCA. It was later shown that the RNA molecules were being selectively incorporated into the prion particle and acquired partially nuclease-resistance upon incubation with PrP[78]. In a recent report, highly infectious recombinant PrP was obtained when a similar mixture containing synthetic lipids (POPG), mice-derived total RNA and recombinant PrP was subjected to PMCA

rounds[83]. Lipids molecules were later shown to exert a combined effect of electrostatic and hydrophobic interactions affecting the acquisition of protease-resistance of recombinant PrP[91]. Therefore, the role of co-factors seems to be essential in modulating some of the most important features of *bona fide* prions, e.g. misfolding and infectivity. On the other hand, recombinant PrP converted into classical amyloids lacks of any detectable infectivity in wild-type animals as well as significant protease-resistance[35, 36, 92]. However, in a recent report, misfolded recombinant PrP acquired variable infectivity and incomplete attack rates when subjected to PMCA in the presence of a non-denaturing detergent (Triton X-100) and a denaturing anionic detergent (SDS)[39]. Although this misfolded PrP showed some biochemical similarities with PrP^{Sc} such as aggregation and self-propagation properties, the proteolytic fragments upon protease-degradation exhibited heterogeneous sizes, indicating a potential difference in the conformation compared to bona fide prions[93].

With the aim of gaining insights into the molecular mechanism underlying PrP misfolding, I tested *in vitro* the role of several molecules on the misfolding of recombinant PrP and further acquisition of protease resistance. I showed that the protease resistance property is reversibly modulated by synthetic accessory organic molecules in a specific fashion. These samples were also injected into wild-type mice in order to correlate infectivity with biochemical properties regarding the role of co-factor on prion propagation.

4.3 RESULTS

4.3.1 Spontaneous formation of protease-resistant recombinant PrP in the presence of detergents. The formation of PrP fragments spanning from residue 90 through 230 represents a key hallmark in prion biochemistry[5]. It has been reported that reactions containing hamster-derived recombinant PrP supplemented with 0.1% Triton and 0.1% SDS generate protease-resistant fragments of PrP when the reactions are seeded with small amounts of bona fide hamster PrP^{Sc} [38]. These C-terminally truncated fragments exhibited sizes of around 10, 12 and 16 kDa, being the latter reminiscent of that observed upon digestion of PrP^{Sc}. In a follow-up work it

was shown that in the absence of prion seeds, small amounts of lower molecular weight fragments (between 10-12 kDa) formed spontaneously in a temperature-dependent manner[44]. I adapted this protocol to use it with mouse recombinant PrP and found a similar phenomenon (Fig. 4.1). However, I observed that at higher temperatures and using different reactions tubes, the formation of the prion-related degradation band was clearly enhanced (Fig. 4.1B). At 37°C, the frequency of spontaneous generation of protease resistant species was lower than that at 50°C. (Fig. 4.1A). More importantly, I observed that the reactions incubated at 37°C promoted the formation of lower molecular weight fragments in the range between 10-14 kDa.

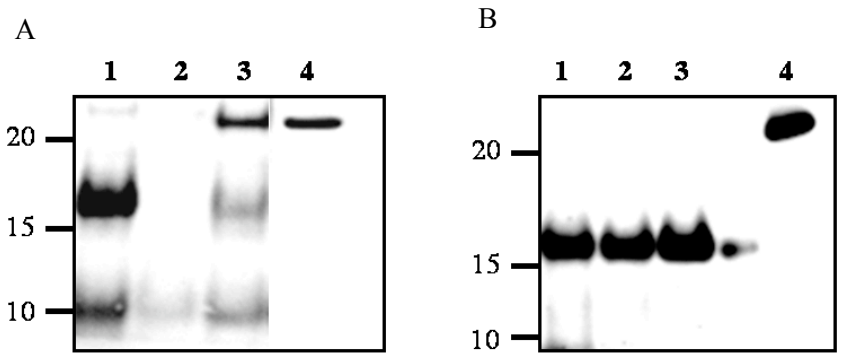

Figure 4.1: *Temperature-dependent spontaneous formation of protease-resistant recPrP.* recPrP was incubated for 24 hrs at 37°C (A) and 50°C (B) as described in methods. Samples were digested with proteinase K for 1 hr at 37°C and western-blotted using mAb 6D11. The experiments were run in triplicate (lanes 1, 2 and 3) to test for sampling. Undigested recPrP is shown in lane 4.

4.3.2 The formation of spontaneous protease-resistant PrP is time-dependent. I next tested whether the formation of protease-resistant PrP followed a time-dependent mechanism. I performed serial passages of 24-hrs-rounds of reactions as described in methods. Since the formation of species resistant to protease degradation exhibited a stochastic fashion, I used several replicates on each round. Upon serial passages of the initial material, the intensity of the bands associated to protease-resistant recombinant PrP fragments increased significantly (Fig.

4.2). At the 22nd passage, the intensity was much higher than that observed in initial passages, and the 16 kDa fragment remained the main species observed after digestion when using monoclonal antibody 6D11 (Fig. 4.2A).

A

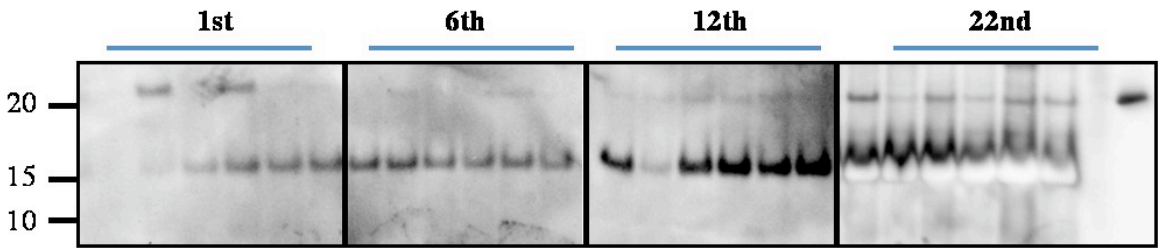

B

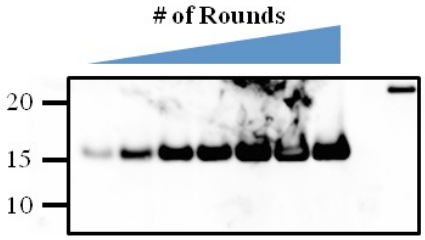

Figure 4.2: *Time-dependent formation of protease resistant recPrP.* recPrP was incubated for 24 hrs at 50°C as described in methods and then subjected to 22 cycles of amplification by using 1/10th of the previous reaction as seeding material for the next round of amplification. Samples were digested with proteinase K for 1 hr at 37°C and western-blotted using mAb 6D11. Six replicates were prepared in each round. Rounds 1st, 6th, 12th and 22nd are shown in A. Combined rounds of one of the replicates are shown in B. Undigested recPrP is shown in the last lane (A and B).

4.3.3 The main proteolytic products are C-terminal recombinant PrP fragments. PrP^{Sc} is known to exhibit protease-resistance from residues ~90 to the very end of the C-terminal region of PrP[5, 88]. In order to perform a molecular profiling of the spontaneously-generated recPrPres, I

used a monoclonal antibody that reacts against a region within the C-termini of PrP (M-20). The 16 kDa band reacted positively with both 6D11 and M-20 antibodies, confirming that this proteolytic product is a C-terminal fragment (Fig. 4.3). However, I also observed several lower molecular weight bands using the M-20 but not the 6D11 antibody (Fig. 4.3A). These bands have approximate molecular weights ranging between 10-12 kDa and appeared in lower amounts than the 16 kDa fragments. These bands were also reported in the work mentioned above upon conversion of hamster recPrPs, though in that case the 16 kDa band was barely identifiable[44]. In order to further study the time-dependent formation of these proteolytic fragments, a time-course experiment of conversion of recPrP was analyzed by using M-20 antibody (Fig. 4.3B). These results revealed that the lower molecular weight bands started forming in earlier passages, whereas the 16 kDa band exhibited a more time-dependent behavior achieving increasing amounts upon passages.

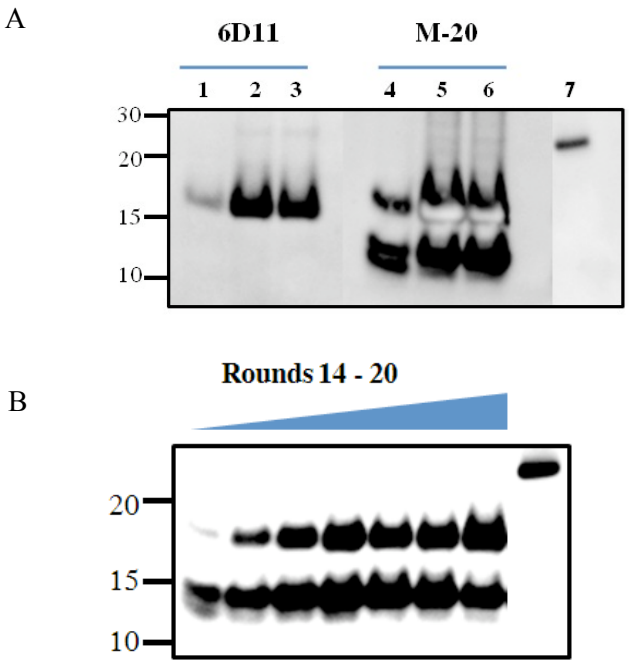

Figure 4.3: *Antibody mapping of protease resistant recPrP.* recPrP was incubated for 24 hrs at 50°C as described in methods. Samples were digested with proteinase K for 1 hr at 37°C. A)

Samples were western-blotted using two different antibodies: 6D11 (region 95-105) and M-20 (C-terminal mAb). Triplicates of the reactions were digested at a PK/recPrP ratio of 1/5 (lanes 1 and 4) and 1/40 (lanes 2, 3, 5 and 6) respectively. Undigested recPrP is shown in lane 7. B) Time- course experiment for spontaneous formation of recPrPres followed by M-20 mAb. Undigested recPrP is shown in last lane.

4.3.4 The formation of the 16 kDa but not the smaller protease-resistant PrP fragment is reversible. In order to gain more insights about the nature of the protease-resistant PrP fragments formed spontaneously upon incubation, I proceeded to analyze the role of the solution components on the recPrP features. Due to the insoluble nature of misfolded recPrP, the aggregates formed upon passage 22nd were centrifuged and washed with PBS in the absence of any other additive. This step was repeated until no visible signs of detergents were observed. After final resuspension in PBS, I submitted the samples to protease-degradation assay. Surprisingly, the 16 kDa fragment was barely visible after the washing steps (Fig. 4.4A lane 3). However, at lower protease concentrations, the fragment reappeared with a stronger signal (Fig. 4.4A lane 1). When the washed samples were probed with the M-20 antibody, I observed the same phenomenon with the 16 kDa fragment, but the lower molecular weight fragments remained unaffected by the washing steps (Fig. 4.4B lanes 1 and 2). Once the detergents were added back to the washed pellets, the recovery in signal of the 16 kDa fragment reached similar levels as those shown initially (Fig. 4.4A lanes 2 and 4, Fig. 4.4B lanes 3 and 4). Interestingly, upon detergent addition only one band at around 12 kDa was observed in addition to the 16 kDa band. Altogether, these results suggest that the 16 kDa fragment is modulated by the presence of the reaction additives, e.g. SDS and triton, as opposed to the lower molecular weight fragments.

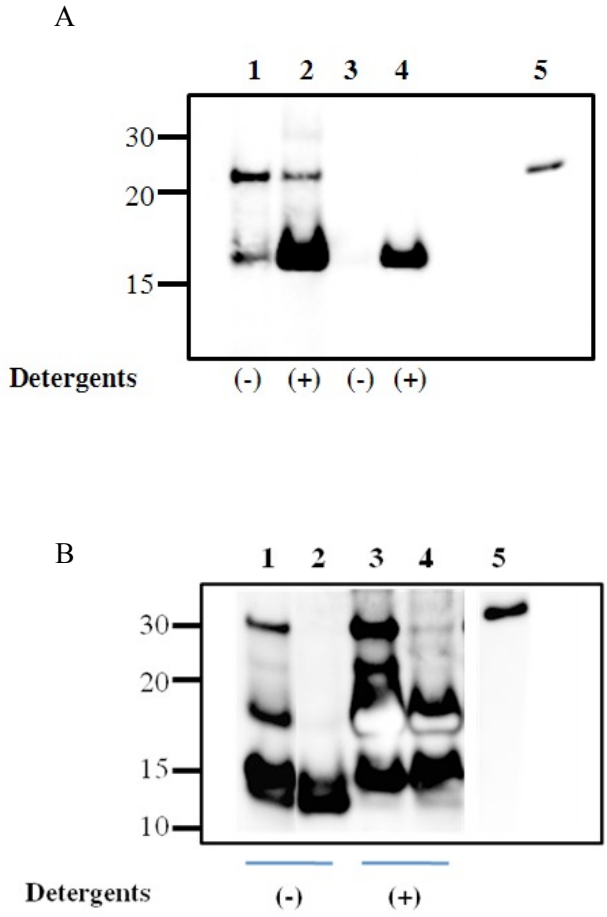

Figure 4.4: *Protease resistance of PBS–washed PrP aggregates.* recPrP was spontaneously converted into recPrPres as described in Fig 4.1. Aggregated recPrP from round 22 was exhaustively washed with saline buffer (PBS) to remove reaction detergents, as described in methods. A) recPrP pellet was resuspended in PBS (-) or PBS plus reaction detergents (0.1% Triton X-100 and 0.1% SDS, (+)), incubated at 37°C for 1 hrs and then protease-digested for 1 hrs at 37°C at 1/10 (lanes 1 and 2) and 1/40 (lanes 3 and 4) PK/recPrP ratios. Samples were western-blotted using 6D11. B) recPrP pellet was resuspended in PBS (-) or PBS plus reaction detergents (0.1% Triton X-100 and 0.1% SDS, (+)), incubated at 37°C for 1 hrs and then protease-digested for 1 hrs at 37°C at 1/10 (lanes 1 and 3) and 1/40 (lanes 2 and 4) PK/recPrP ratios. Samples were western-blotted using M-20.

4.3.5 Effects of different detergents on the formation of the 16 kDa protease-resistant PrP fragment. I previously observed that detergents seem to modulate the formation of the 16 kDa fragment. As a next step I checked the individual effect of SDS and Triton on the washed pellets. Interestingly, none of these detergents were able to recover the 16 kDa band upon addition to the pellets (Fig. 4.5A). As it was shown, the combination of both seems the only way to retrieve the original levels (Fig. 4.4B lanes 3 and 4). In addition, the lower molecular weight fragments were observed throughout all the experiments. In order to further dissect the role of detergents, two additional anionic detergents were tested. I first tried deoxycholic acid, a negatively charged non-denaturing detergent broadly used to solubilize membrane proteins. Upon addition to the pellets, deoxycholic acid was not able by itself to recover the 16 kDa-associated signal, even at high concentrations (Fig.4.5B). Next I tried Sarkosyl, a negatively charged detergent similar in chemical structure to SDS but without protein-denaturing effects (Fig.4.5C). Surprisingly, the 16 kDa band associated to protease-resistant recPrP was fully recovered. Moreover, the effect of Sarkosyl followed a clear concentration-dependence trend, increasing the amount of the fragment to much higher levels than that initially observed (compare Fig. 4.4B lanes 3 and 4 with Fig.4.5C lanes 3-6). Different PK concentrations had minimal effect on the intensity associated to the 16 kDa band. In addition, this band was evidently the main species remained upon digestion. When I tried even higher ratios of PK/recPrP (1/1), the band remained completely visible whereas the lower molecular weight fragments disappeared (Fig.4.5A lane 4). As a comparison, I performed the same experiment but using SDS instead. Though not so chemically distant in structure, SDS was not able to stabilize this band against degradation (Fig. 4.5A lane 6). These results suggest that a negatively charged polar head is not enough to recover the PrP^{Sc}-like protease resistant feature. In order to fully test that, I incubated the washed pellets at high concentrations of NaCl. Again, the 16 kDa was not visible (Fig.4.5D).

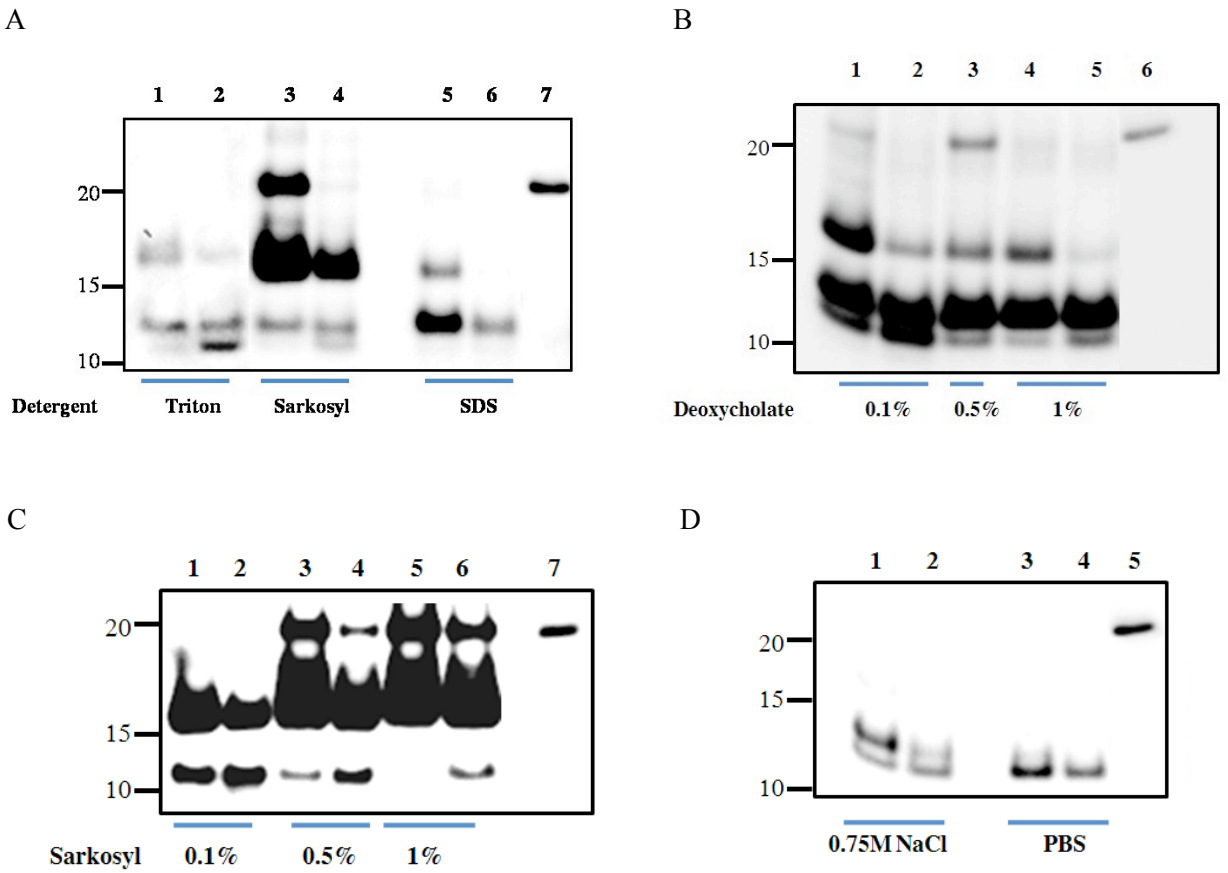

Figure 4.5: *Effect of detergent co-factors on recPrP protease-resistance.* recPrP was spontaneously converted into recPrPres as described in Fig. 4.1 and the aggregates from round 22 were exhaustively washed with saline buffer (PBS) to remove reaction detergents, as described in methods. RecPrP pellet was resuspen

ded in different detergents or co-factors, incubated at 37°C for 1 hrs and submitted to protease digestion assay, followed by Western blotting and visualized by using C-terminal mAb M-20. A) Effect of resuspension in PBS plus: 1% Triton X-100 at PK/recPrP ratio of 1/10 and 1/1 (lanes 1 and 2), 1% Sarkosyl at PK/recPrP ratio of 1/10 and 1/1 (lanes 3 and 4) and 1% SDS at PK/recPrP ratio of 1/10 and 1/1 (lanes 5 and 6). B) Effect of different concentrations of deoxycholate detergent at PK/recPrP ratio of 1/40 (lanes 1, 3 and 4) and 1/10 (lanes 2 and 5). C) Effect of different concentrations of Sarkosyl detergent at PK/recPrP ratios of 1/40 (lanes 1, 3 and 5) and 1/10 (lanes 2, 4 and 6). D) Effect of NaCl (0.75M) compared to PBS resuspension at PK/recPrP

ratios of 1/40 (lanes 1 and 3) and 1/10 (lanes 2 and 4). Undigested recPrP is shown in lanes 8 (A), 7 (B), 6 (C), 7 (D) and 5 (E).

4.3.6 Effect of poly-adenine (Poly-A) RNA on the aggregation of recombinant PrP . It has been reported that poly-anions, particularly large fragments of RNA poly-adenine molecules strongly stimulate formation of PrP^{Sc} [72, 94]. Moreover, brain-purified PrP was spontaneously converted into an infectious form when a mixture containing poly-A plus co-purifying lipids [73, 78], as well as mouse recombinant PrP when combined with mouse-extracted total RNA and synthetic lipids, was submitted to cyclic amplifications rounds (PMCA)[83]. Using washed pellets of previously converted recPrP, I tested the effect of synthetic poly-A in the restoration of the protease-resistant 16 kDa fragment. RNA alone was not able to recover the signal (Fig.4.6A lane 7). However, when combined with Triton X-100, the signal reached similar levels to those initially observed (Fig.4.6A lanes 5 and 6). RNA combined with Sarkosyl did not increase further the signal obtained with the detergent alone (data not shown). In order to gain more insights about the role of RNA (poly-A), I added poly-A molecules during the conversion of recPrP from the first round. As controls, I also included other polyanionic molecules in separate reactions: polyglutamate (poly-E) and polyvinyl-sulfate (poly-S). Surprisingly, after 18 rounds of reaction I observed an intense signal associated to the 16 kDa fragment in the reaction supplemented with poly-A, but not in those with poly-E or poly-S (Fig.4.6B). Moreover, the signals of the lower molecular weight fragments were much weaker compared to that of the 16 kDa fragment, and also compared to the fragments obtained in reactions without poly-A (compare Fig. 4.3A with Fig.4.6B lanes 1 and 2).

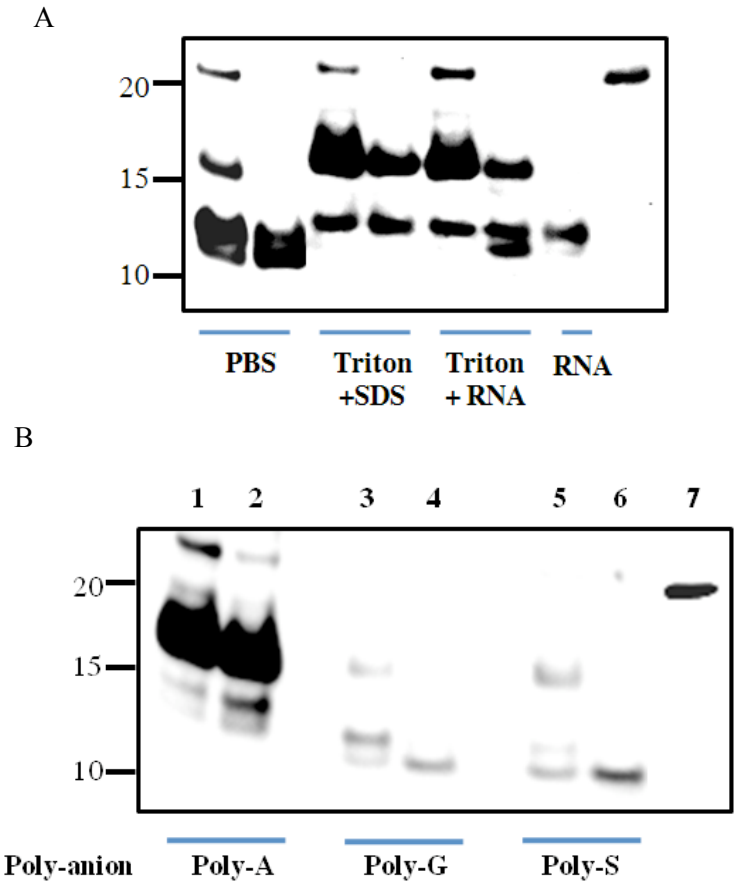

Figure 4.6: *Effect poly-anions on spontaneous formation of recPrPres.* A) Effect of resuspension of washed recPrP aggregates in: PBS at PK/recPrP ratio of 1/40 and 1/10 (lanes 1 and 2), reaction detergents (0.1% Triton X-100 and 0.1% SDS plus PBS) at PK/recPrP ratio of 1/40 and 1/10 (lanes 3 and 4), reaction detergents without SDS plus RNA (0.1% Triton X-100) at PK/recPrP ratio of 1/40 and 1/10 (lanes 5 and 6) and PBS plus RNA at PK/recPrP ratio of 1/40 (lane 5). Undigested recPrP is shown in lane 8. B) recPrP was incubated for 24 hrs at 50°C and subjected to 18 cyclic amplification rounds as described in methods, in the presence of different poly-anionic molecules: poly-adenine RNA (poly-A), poly-glutamate (poly-E) and poly-vinyl-sulfate (poly-S). Protease-digested samples at PK/recPrP ratios of 1/40 (lanes 1, 3 and 5) and 1/10 (lanes 2, 4 and 6) were Western-blotted using mAb M-20. Undigested recPrP is shown in lane 7.

4.3.7 Protease-resistance analysis of RNA-induced conversion of recombinant PrP. In order to gain more insights into the role of RNA in the increased formation of protease-resistant, PrP^{Sc}-like recPrP fragments, as described above, I further analyzed their protease-resistance features by conducting a PK concentration-dependence experiment using RNA-induced and non RNA-induced misfolded recPrP. As shown previously, lower PK/recPrP ratios gave protease-resistant fragments mainly around 16 kDa, specially for RNA-induced conversion reactions, whereas lower molecular weights species appeared in lower proportions (Fig.4.7A and 4.7B). On the contrary, the intensity of the 16 kDa band formed in the absence of RNA showed a higher sensitivity against PK (Fig. 4.7C and 4.7D). The lower molecular weight bands clearly increased with higher PK/recPrP ratios (Fig.4.7D). A side-by-side analysis about the extent of protease-resistance of both RNA and non-RNA generated recPrPres exhibited clear differences (Fig. 4.7E). The non RNA-induced reactions gave aggregates with an increased sensitivity to higher PK/recPrP ratios, with the 16 kDa band almost disappearing at the highest PK concentrations (Fig.4.7E). The similar intensity of the 16 kDa bands at PK/recPrP ratios of 5/1 and 4/1 for RNA-induced and non-RNA induced reactions respectively enabled me to estimate that RNA-induced reaction products are at least 20 times more protease-resistant than those in the absence of RNA. Interestingly, the lower molecular weight bands exhibited some RNA-dependent size differences (Fig. 4.7E). In order to further confirm this, I run the same samples in higher-concentration acrylamide gels (12%) to fully resolve the band separation. As shown in Fig.4.7F, the RNA-induced products clearly contained a larger proteolytic fragment than that of the non-RNA-induced reaction (besides the 16 kDa fragment). In both reactions, the lower molecular weight fragments started increasing in signal when higher PK/recPrP ratios were used, suggesting a potential involvement in the formation and/or proteolytic processing of the larger, 16 kDa protease-resistant species (Fig.4.7E).

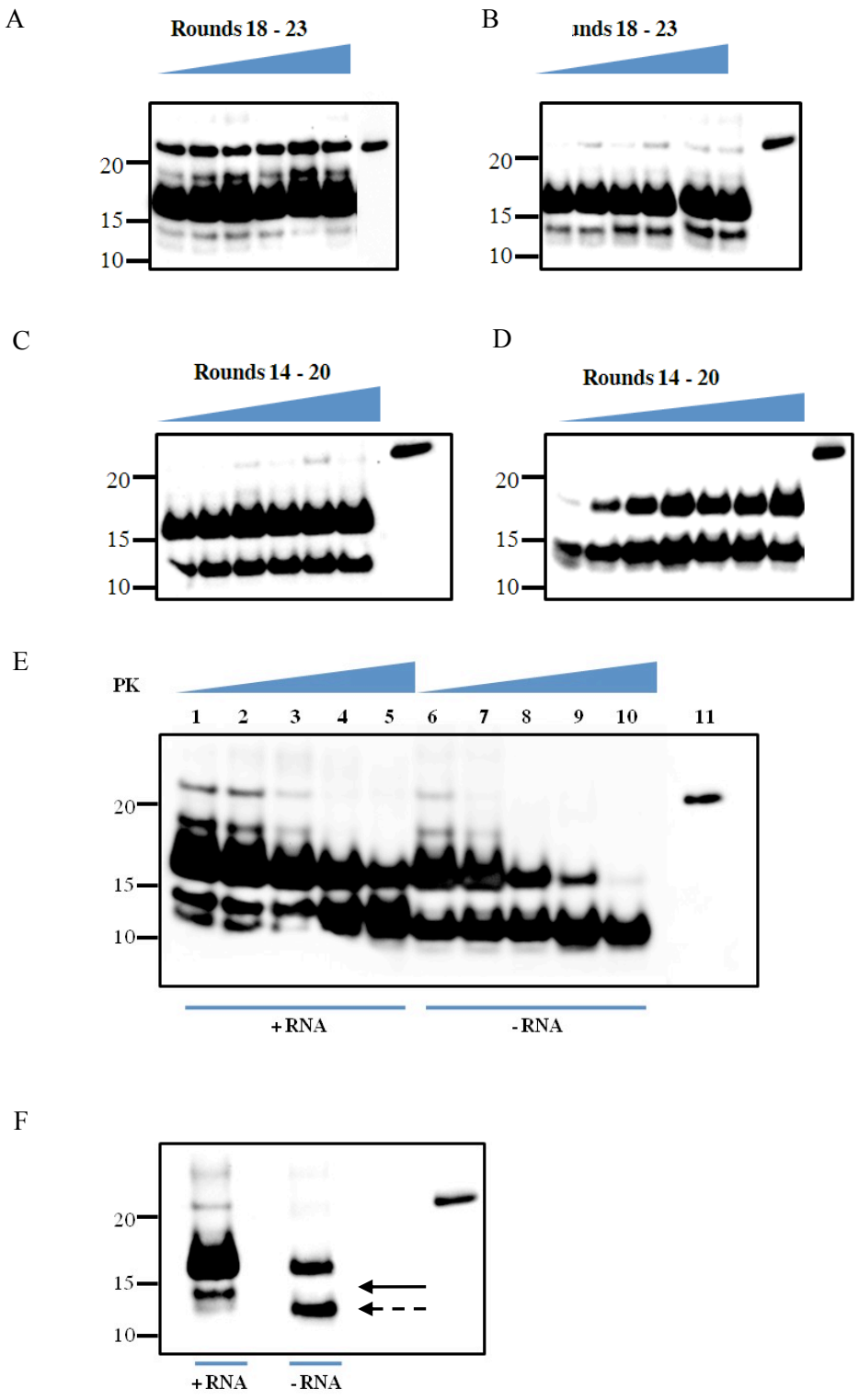

Figure 4.7: *Comparison between RNA-dependent and RNA-independent spontaneous formation of recPrPres.* recPrP was incubated for 24 hrs at 50°C and subjected to cyclic amplification rounds as described in methods, in the presence or absence of poly-adenine RNA, followed by

Western-blotting and analyzed by mAb M-20. A and B) Amplification rounds from 18-23 in the presence of poly-A are shown at PK/recPrP ratios of 1/40 (A) and 1/10 (B). C and D) Amplification rounds from 14-20 in the absence of poly-A are shown at PK/recPrP ratios of 1/40 (C) and 1/10 (D). E) Aggregated recPrP formed in the presence (+RNA) or absence (-RNA) of poly-A RNA from round 20 was protease-digested at PK/recPrP ratios of 1/90 (lanes 1 and 6), 1/40 (lanes 2 and 7), 1/10 (lanes 3 and 8), 1/1 (lanes 4 and 9) and 5/1 (lanes 5 and 10). F) Protease-digested aggregated recPrP at PK/recPrP ratios of 1/10 in the presence (+RNA) or absence (-RNA) run in 12% acrylamide SDS-PAGE followed by Western-blotting. The solid arrow indicates the lower molecular weight size fragment (~13-14 kDa) of the RNA-induced recPrPres compared to the non-RNA recPrPres fragment of around 12 kDa (dashed arrow). Undigested recPrP is shown in the last lane of all figures.

4.3.8 Infectivity of aggregated recPrP in the presence of different co-factors. In order to test the self-propagation and infectivity of the aggregated recPrP described in the previous sections, I inoculated these samples intra-cerebrally into wilt-type mice as described in Table 1. The starting material was aggregated recPrP in the presence of 0.1% SDS and 0.1% Triton in PBS, as described in methods and shown in figure 4.1. Then, I exhaustively washed these aggregated recPrP sample using PBS, as described previously and in methods. The washed aggregates were resuspended in different buffers, checked for PK-resistance and then injected into animals, as described in Table 1. For a second group of injections, I resupended the washed pellets in the original buffer (0.15 SDS and 0.1% Triton in PBS) and then incubated the suspension with several "inorganic" material that are known to affect prion propagation *in vivo*: stainless-steel wires and nitrocellulose[95-97]. These samples were directly inoculated into mice. The infectivity studies with these samples are currently ongoing.

Mice group	*Inoculums injected intra-cerebrally*
1	***PBS***
2	***0.1% SDS + 0.1% Triton X-100 in PBS***
3	***0.5% Sarkosyl in PBS***
4	***0.1% SDS + 0.1% Triton X-100 + poly-A in PBS***
5	***0.1% SDS + 0.1% Triton X-100 in PBS – Stainless steel wires***
6	***0.1% SDS + 0.1% Triton X-100 in PBS – Nitrocellulose***

Table 1: *Description of samples inoculated intra-cerebrally into wild-type mice*. RecPrP was aggregated as shown in Fig. 4.1 and exhaustively washed against PBS. The pellets were resuspended in different solutions as specified in the second column followed by overnight incubation at 37°C. The resulting samples were intra-cerebrally injected into the hippocampal brain region. Ten mice per group were inoculated. Solutions devoid of PrP were also injected as experimental controls.

4.3.9 Surface electrostatic potential of a putative PrP^{Sc} structural model. As mentioned in chapter 1, high-resolution structural data of bona fide PrP^{Sc} is not yet available. Therefore, several theoretical models have been proposed based on experimental data[98-100]. Of those, the most accepted in the field was reported in 2001 and proposes a b-helix arrangement for the minimal structural PrP^{Sc} unit (Fig. 4.8C, with permission from Holger Wille)[99]. Since my previous results suggest altogether that negatively-charged molecules play an important role on the conversion of recPrP, I run surface electrostatic potential calculations on the b-helix model for mouse PrP^{Sc} (Fig.4.8). Interestingly, the results showed a major spatial rearrangement of both positive and negative charges in the region corresponding to the b-helix (residues 90-145) compared to soluble recPrP structure[14] (Fig.4.8). Moreover, the positively-charged face seems to expose a considerably larger electrostatic area than the negatively-charged face, suggesting a

possible role for the involvement of negatively-charged molecules on PrP conversion studied here.

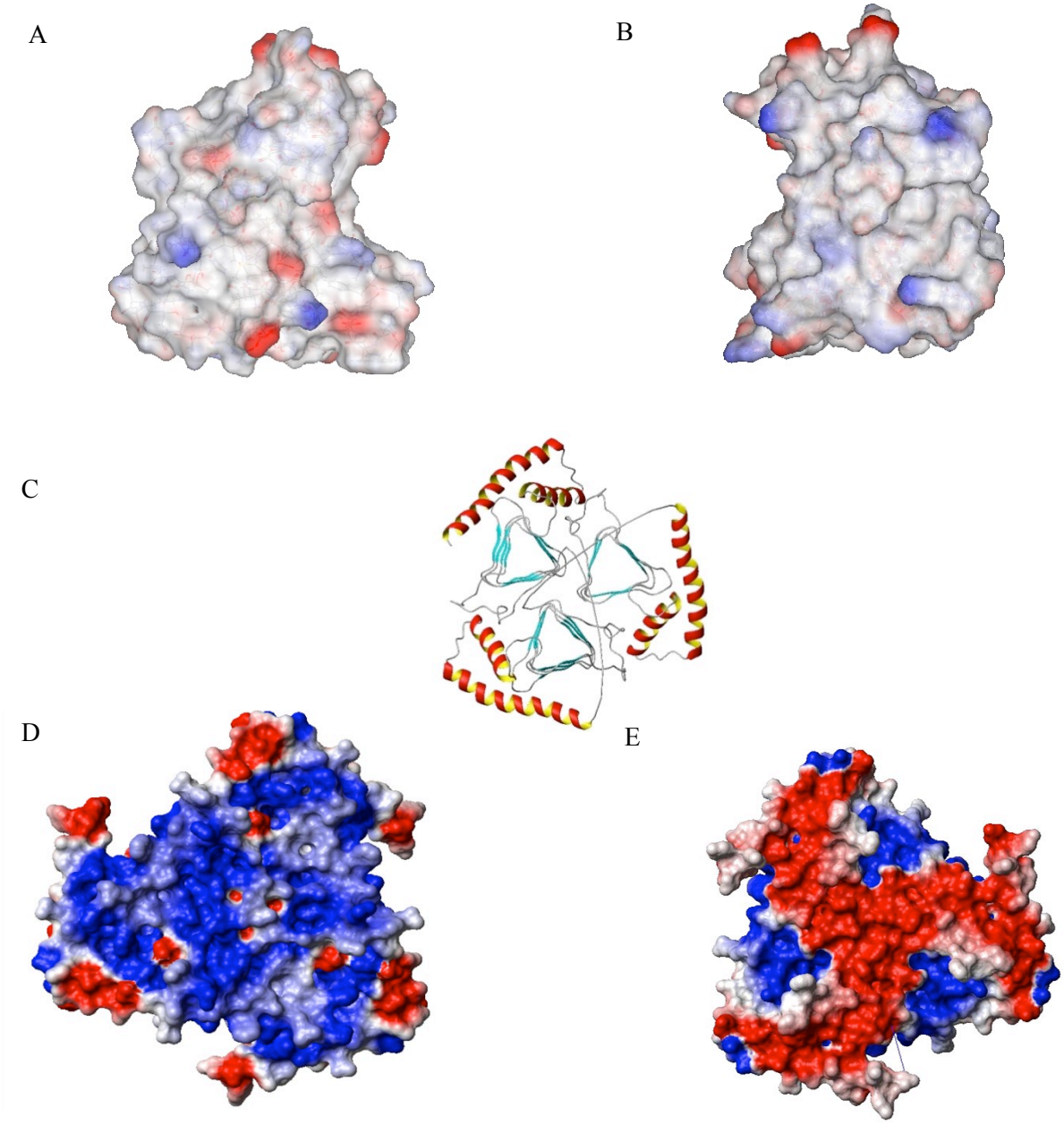

Figure 4.8: *Surface electrostatic potential of PrP*. Calculations of electrostatic potential for different PrP structures at physiological pH and temperature was performed using MolMol software's surface potential application. A and B) Electrostatic surface potential front side (A) and back side view (B) of normally folded mouse PrP X-ray structure (PDB access 1AG2). C)

Trimeric model of PrP^{Sc} minimal structural unit provided by William Holger[92]. D and E) Electrostatic surface potential front side (D) and back side view (E) of trimeric PrP^{Sc} model shown in C.

4.4 DISCUSSION

Accessory molecules have recently gained attention due to their potential role in the misfolding process of PrP into PrP^{Sc}[72, 73, 83]. The generation of infectious prions using brain-derived PrP[73] and recombinant PrP[83] has provided strong evidence against an exclusively-protein hypothesis about the formation of prions. However, the role of these co-factor molecules is not yet clear. Lipids and RNA have consistently shown to promote prion-like features, suggesting a role for negatively charged groups and hydrophobic interactions[56, 101-105]. In a recent report, prion-like particles with highly heterogeneous infectivity and incomplete attack rates were generated using only synthetic detergents and cyclic amplification[39], blurring even further the role of these co-factors. In that work, aggregated recPrP seeded with bona fide PrP^{Sc} was shown to be infectious upon intra-cerebral injection into wilt-type hamsters. The reaction conditions used in that work included 0.1% SDS and 0.1% Triton in PBS[44]. In this chapter, I studied the effect of these and other detergents as well as several poly-anionic molecules on the formation of protease-resistant recPrP in unseeded reactions, e.g. recPrPres formation *de novo*, which has the advantage of avoiding brain-derived contamination. These samples were further bioassayed in wild-type mice to correlate the findings *in vitro* with results *in vivo*.

Co-factor mediated in vitro conversion of PrP. I initially found that a partially protease-resistant PrP species with features of PrP^{Sc} is spontaneously generated upon incubation in a mixture of detergents submitted to amplification cycles (Fig. 4.1). The formation of these particles was time and temperature dependent with a relatively linear correlation, probably reflecting a kinetically constrained process as has been suggested previously[40] (Fig. 4.2). A mayor protease-resistant 16 kDa band, reminiscent of GPI-anchor-less, unglycosylated PrP^{Sc} [5, 54] appeared after several rounds of amplification (Fig. 4.1B). At 37°C, smaller molecular weight

bands were also visible (Fig. 4.1A). These bands were positive when using the monoclonal antibody 6D11, which reacts against an epitope located at 95-105 in PrP. When comparing the expected size for a fragment containing that epitope (Fig. 4.10), these results indicate that the protease degradation occurred at both the C-termini and the N-termini, as opposed to what is seen with PrP^{Sc88}. On the other hand, the reactions submitted at 50°C gave only a protease-resistant band weighing around 16 kDa by using the same antibody, and a C-terminal antibody (Fig. 4.3A), suggesting that at this temperature the PrP^{Sc}-like fragments are clearly enhanced (Fig. 4.1B and Fig. 4.10). In further experiments, I found that the 50°C generated recPrP species also exhibited PK-resistant fragments of lower sizes, which were reactive against the C-terminal-directed antibody M-20 as opposed to the smaller fragments formed at 37°C (Fig.4.3A). The sizes of these fragments suggest that degradation of PrP went further down residue 90, leaving smaller fragments resistant to proteases (Fig. 4.10). These fragments are not usually observed with bona fide PrP^{Sc}, though some variants of Creutzfeld-Jacob disease and Scrapie have clearly exhibited C-terminally truncated $PrP^{Sc\ 106\text{-}108}$. In the present study, a previously reported experimental protocol was adapted to enhance the spontaneous rate of PrP^{Sc}-like particles[44]. In that report, the same bands were also observed. It is not yet clear whether the formation of these bands is related to a further processing of the 16 kDa, PrP^{Sc}-related species, or rather a separate population. However, the fact that degradation occurs all the way up to residues surrounding the folded C-terminal domain (Fig. 4.10) may be indicative of destabilization of a protease-resistance conformation acquired upon misfolding of this originally natively unfolded zone 90-135. Ongoing experiments are aimed to distinguish these possibilities.

The yield of spontaneous formation of recombinant PrP fragments resistant to proteases was relatively low compared to total PrP in the reaction (data not shown). This means that only a small fraction of recombinant PrP is converted to a PrP^{Sc}-like species. I observed some visible aggregation and sometimes precipitation of protein after 1 round reaction (data not shown). This is consistent with a scenario in which most PrP follows aggregation pathways, but only a fraction acquires protease-resistance features reminiscent of bona fide prions[40]. I found that the relative

amounts of the 16 kDa protease-resistant fragment were highly dependent on the presence of detergents (Fig. 4.4). Though neither SDS nor Triton X-100 was able to individually recover the formation of these bands after exhaustively washing the recPrP aggregates, a combination of both regained the initial levels (Fig.4.4 and 4.5A). When Triton X-100 was combined with RNA, a similar recovery was obtained (Fig. 4.6A), whereas Sarkosyl by itself recovered not only the initial levels, but also acted in a concentration-dependent manner, reaching higher levels of protease-resistance (Fig. 4.5C). An alternative explanation is that Sarkosyl and other detergents may inhibit protease activity. However, proteinase K (PK) is known to be fully active in Triton X-100 (up to 1%), SDS (up to 1%) and also Sarkosyl (up to 1%)(see proteinase K datasheet from QIAGEN and SIGM-ALDRICH). These results suggest that a molecule containing a negatively charged group and a hydrophobic moiety are at least required to achieve a PrP^{Sc}-like conversion, which is consistent with recently reported data[91]. The fact that SDS and RNA did not have significant effects when used separately but only when combined with Triton X-100 suggests that they may convey a similar role, probably by providing negative charges required for a putative conformational change, whereas Triton X-100 may provide a hydrophobic environment. Triton and lipids have shown to exhibit complementary effects on PrP conversion before[56]. On the other hand, Sarkosyl may convey both requirements in a single chemical setup. Interestingly, Sarkosyl is routinely used in purification and enrichments protocols of PrP^{Sc} fractions at even very high concentrations, suggesting that PrP^{Sc} is clearly Sarkosyl-compatible[5, 25]. Moreover, Sarkosyl molecules are normally found on highly purified extracts of PrP^{Sc} even after thorough washing steps, suggesting high affinity binding to the infectious form[109]. Though not significantly different in structure than SDS, Sarkosyl is usually regarded as a non-denaturing detergent, which may be a key difference in the opposite effects both detergents exhibited (Fig. 4.9). The hydrophobic requirement in PrP conversion may be related to an increase in the aggregation state of the protein, as proposed before[56, 91]. The hydrophobicity of SDS molecules is either incompatible in promoting PrP aggregation in the levels that Triton X-100 promotes, or its chain may exert more detrimental effects on PrP conversion such as excessive denaturation than

in presence of Triton X-100 are partially counteracted by an aggregation-directed stabilization of PrP aggregates.

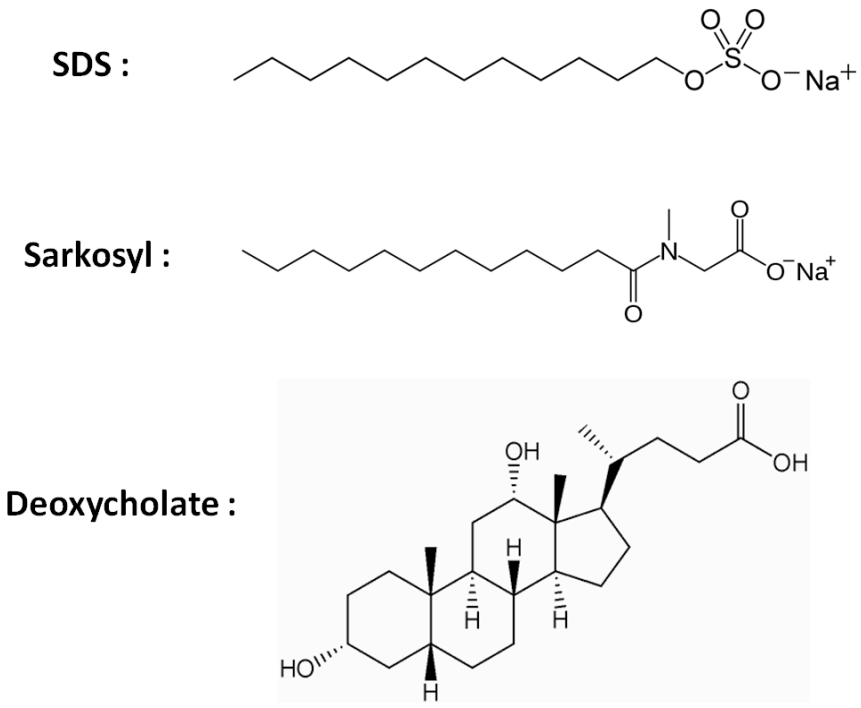

Figure 4.9: *Chemical structure of detergents.* Structures were taken from Wikipedia.org.

When RNA was included in the reaction since the first passage, I observed the formation of seemingly larger amounts of protease-resistance fragments compared to those in the absence of RNA at the same PK and total protein concentrations (Fig. 4.7A and 4.7B compared to 4.7C and 4.7D). At least three possible scenarios are possible: 1) a different, more protease-resistant species is formed when RNA is included in the initial reaction; 2) RNA itself makes the recPrP aggregates more protease-resistant; 3) RNA significantly increases the amount of PrP^{Sc}-like protease-resistant fragments, e.g. yield of the reaction. It is yet unclear which scenario is correct.

However, the fact that the lower molecular weights fragments generated upon PK treatment (~10-12 kDa) migrated slightly slower compared to non-RNA incubated reactions (Fig. 4.7E and 4.7F), provides evidence that a different processing and consequently PrP misfolded form might be taking place.

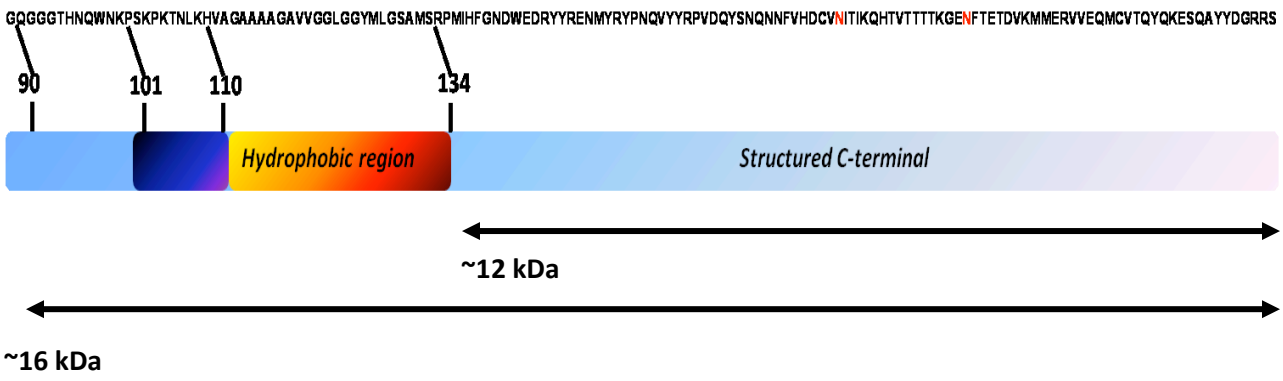

Figure 4.10: *Sequence analysis of PrP.* The different regions of PrP from residues 90-230 (minimal fragment required for infectivity[89]) are described. The globular C-terminal domain spanning from residues 134-230 is represented in light blue. Residues 90 to 134 are structurally disordered in normally folded PrP[14, 110]. A hydrophobic set of residues (11-134) is highlighted in yellow-to-red gradient. A positive cluster of lysines is depicted in dark blue. The arrows represent the estimated linear molecular weight size of the respective region.

In any case, the results I found reflect that the formation of a PrP^{Sc}-like protease-resistant fragment is highly dependent on the electrostatic and hydrophobic character of the surroundings, which is in agreement with the requirement of lipids and RNA to obtain infectious synthetic prions[73, 83]. My observations that the appearance of the 16 kDa, PrP^{Sc}-like protease-resistant fragment, and not the smaller fragments, is reversibly controlled by the molecules studied here, suggest at least two possible mechanisms: 1) this species is always present in the reaction even

after thorough washes but its stability against degradation is mainly controlled by the properties of the co-factor molecules and their affinity to PrP aggregates; 2) the acquisition of protease-resistance in the region between ~90-140 which mostly contributes to the extension of the PrP protease-resistance core starting at the C-termini is related to a reversible conformational change primarily controlled by the co-factor molecules. I am currently testing these hypotheses. In summary, the fact that PrP^{Sc}-like features are modulated by other molecules after thorough washing steps of the pellets, provides evidence for a very tight molecular relationship between PrP^{Sc} and accessory co-factors.

***In vivo* studies and implications**. All of the samples described in this chapter were intra-cerebrally inoculated in wild-type mice in order to test the *in vivo* ability of recPrP-co-factor aggregates to self-propagate. Though these experiments are currently ongoing, several scenarios can be envisioned. As suggested in chapter 1 and in a recent report[41], an accessory molecule can be essential in driving the misfolding of PrP (Fig. 1.2 B, C and E). Biochemically, I described in this chapter that several detergents and negatively charged groups can reversibly modulate the formation of a PrP^{Sc}-like protease-resistance fragment. The reversibility of this process is more in agreement with the aforementioned driving of PrP misfolding. However, infectivity studies are required to confirm this. Previous studies have shown that stainless-steel and nitrocellulose can have effects on prion infectivity when combined with brain homogenates containing cellular PrP[95, 97]. These co-factors can be considered unspecific carriers of prions. I also tested this scenario by combining aggregated recPrP with both materials followed by bioassays (Table 1). If significant infectivities are found with these inoculates, then the role of co-factors will be more related to a stabilization of aggregated recPrP upon inoculation rather than conformational induction, as depicted in Fig. 1.2D.

CHAPTER 5

GENERAL CONCLUSION

The elucidation of the molecular basis driving the conversion of a normally folded protein into an infectious, pathological form has constituted a long-sought aim in the field of prions. The unconventional character of such an unusual infectious agent has brought interest not only from the epidemiological point of view but also from the basic science. Before prions were identified, the smallest infectious particles known were viruses, which still exhibit classical infectious mechanisms and constitute highly ordered, defined macromolecular assemblies. The radical idea that a protein conformation rather than a nucleotide-based pathogenic agent can become infectious and be fatal in mammals has deeply shaken the foundations of microbiology and protein sciences.

Despite decades have passed since the first case reports and the identification of PrP, the exact molecular nature of prions is still elusive, as well as the toxic species causing neuronal death. Most efforts aimed to uncover the structural aspects of prions have so far failed in providing high resolution details. The main problems to overcome are related to the very nature of prions, such as high insolubility, heterogeneity and large size. One of the crucial questions to address is the identification of the minimal structural unit that is required to cause infection.

Viruses are known to be discrete particles of defined structure composed of protein shells covering nucleotide molecules that are injected into target cells by protein-based motors. There is growing evidence that prions propagate through a nucleation-polymerization mechanism characterized by template-directed misfolding of normally folded PrP[17, 111]. However, the minimal particle required to convey such devastating process is still unknown. Most of the problems are related to the continuous failures in creating exclusively protein-only inoculates that cause infections in wild-type animals[35, 36]. Reconstitution experiments of prion infectivity using defined components have so far able to achieve bona fide prion infectivity only when lipids and RNA molecules are present in the inoculate[73, 83], or variable infectivity with incomplete attack rates when different detergents are used[39]. The clear differential effects observed in both works argue that accessory molecules may be key modulators in prion-like infectivity.

In order to gain more insights about the molecular nature of prions, I designed two different approaches:

1) **Conversion of recombinant PrP into PrP^{Sc}-like forms using salts**: I showed that kosmotropic/stabilizing salts are able to induce formation of protease-resistant recPrP in a concentration and time-dependent manner exhibiting features reminiscent of bona fide prions, such as molecular weight of the proteolytic fragments, amyloid-like nature of aggregates and high content of b-sheet structure, all in a close-to-physiological experimental condition. The fact that simply salts can form PrP species mimicking most biochemical features of prions at physiological pH and temperature suggests that prions are manifestations of protein-related changes. Infectivity studies are ongoing.
2) **Conversion of recombinant PrP into PrP^{Sc}-like forms using organic co-factors**: By modifying previously reported protocols aimed to misfold recPrP using detergents and cyclic amplification, I found that spontaneous formation PrP^{Sc}-like forms in the absence of any seed was significantly enhanced in a temperature and time-dependent fashion.

Moreover, the detergents present in the reactions exhibited a critical role in the formation of PrP^{Sc}-like proteolytic fragments by specifically modulating their molecular weights as well as the level of resistance against protease-mediated degradation. Altogether, these results clearly suggest that a tight relationship between negatively charged molecules combined with specific hydrophobic environment is essential in the misfolding process. Infectivity studies of these samples are ongoing.

Altogether, the results exposed in this thesis work provide support to the idea that prions and their biochemical and pathological features of prions are manifestations of a specific arrangement of PrP and accessory molecules. The fact that recombinant PrP exhibits PrP^{Sc}-like biochemical features only when exogenous components are included in the misfolding reactions as shown in chapters 3 and 4 suggests that prion formation requires either a specific physicochemical environment from which conversion into infectious forms can successfully occur, or specific non-PrP molecules needs to be essentially incorporated within the prion unit in order to form an infectious complex. If salt-induced recPrP aggregates are equally or comparable infectious to those formed in the presence of detergents and negatively charged molecules, then the requirement for co-factor molecules to produce infectious units can be largely relaxed, as depicted in Fig. 1.2B. On the other hand, if significant co-factor dependent effects are observed in vivo regarding infectivity, then the role of accessory-molecules will gain importance, in agreement with the scenarios depicted in Fig. 1.2C-E. Based on the biochemical findings reported in chapters 3 and 4, exogenous molecules seem to convey a critical role in controlling prion formation, in a way that resembles those shown in Fig. 1.2C-E. Further experiments are currently ongoing to discriminate which pathway underlies prion formation.

5.1 A new model for prion formation. The data provided in this thesis work allowed me to hypothesize a new model for prion formation which is also consistent with recently reported findings[73, 83]. The bases for the model are as follows:

Molecular aspects of the model:

A) The acquisition of structure in the 90-145 region is encoded within the primary structure of PrP. The role of cofactor molecules is to further stabilize these strands (Fig. 6.1). The protease-resistance exhibited within the natively unfolded 90-145 region upon PrP misfolding is most likely due to acquisition of a degradation-resistant structure in the form of a b-sheet-like arrangement. The PrP 106-126 segment as well as larger fragments spanning residues within this region has been shown to readily form amyloid-like aggregates *in vitro* with high content of b-sheet signal when expressed separately from the rest of the protein[66, 112-116]

B) The absence of protease resistance within the 90-145 region in exclusively protein-only aggregates [46-49, 117](Fig. 4.4) along with the key modulating role of co-factor molecules in mediating this feature in vitro (Fig. 4.5) suggest that the acquisition of structure within this PrP segment requires further stabilization by non-PrP elements in order to self-sustain. Interestingly, certain lipids such as POPG have been shown to form PrP^{Sc}-like protease resistance PrP species just by short incubation at 37°C [56, 91]. The hydrophobicity-level of PrP itself does not explain the high insolubility of PrP^{Sc}, since monomeric, native PrP remains monomeric at the same concentrations. Consequently, I propose that both non-denaturing hydrophobic environments and negative charges are required to convey protease-resistance (Fig. 4.5). The molecular involvement of accessory molecules is in the form of specific hydrophobic contacts and negatively charged groups. Negative charges are involved in the stabilization of surface-exposed positive charges upon acquisition of structure within the 90-145 region. The hydrophobic interactions proceed through further stabilization of the PrP^{Sc}-conformation by providing a layer-like arrangement of aliphatic groups on the surface of PrP (Fig. 6.1A).

C) The combination of both hydrophobic and negative (non-denaturing) groups is sufficient to stimulate prion like PrP conformations. However, the role of polyanion molecules, especially poly RNA, is not so clear. It has been shown to act as a scaffold of prion formation[45, 73, 78]. Surprisingly, it was recently shown that photo-cleavage of nucleotides bound to PrP^{Sc} did not alter the infectivity, suggesting that once PrP^{Sc} is formed and the polyanion partially incorporated, it is not longer needed by the prion to convey infectivity[118]. Therefore, polyanionic molecules promote in the model a 2D environment for efficient encounter between seed and substrate, most likely through the electrostatic attractions between the negative charges and the highly basic natively unfolded region within monomeric PrP. Hence, the role of polyanions is primarily a catalytic one.

D) During *in vitro* replication, large stacks of misfolded protein are broken up in pieces by external forces such as sonication[33, 73, 83]. In the presence of polyanionic molecules, small seeds can contact monomers in a surface-based catalytic process, accelerating the propagation of prions (Fig. 6.1B).

A

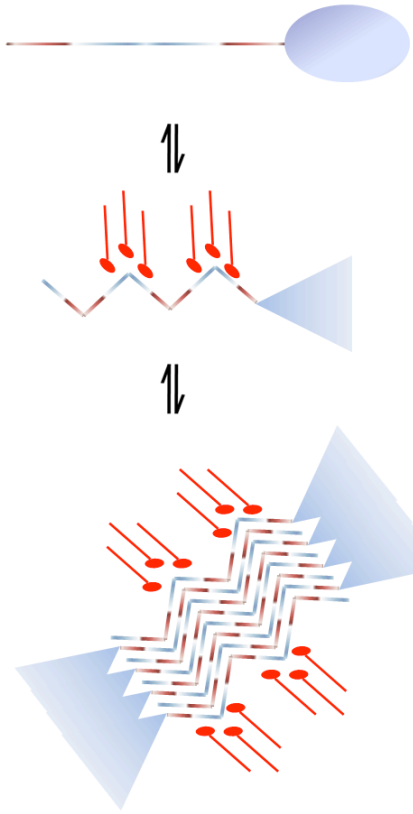

B

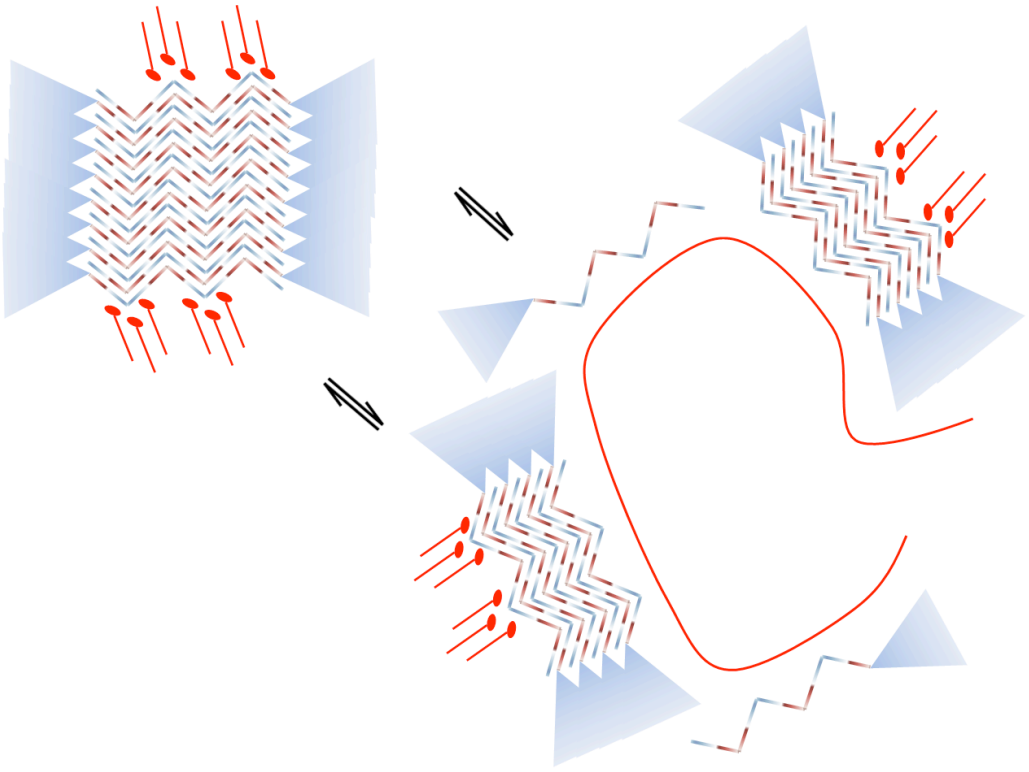

Figure 6.1: *A new model for prion formation and propagation.* A combined role of hydrophobic and negative charges provided by non-PrP components are proposed as essential in the generation of bona fide prions. PrP C-terminal domain is represented as circle (native form) or triangle (misfolded form) while the N-terminal domain (90-145) is depicted as a straight line (natively unfolded) or wavy line (structured form). The N-terminal domain positive side chains are shown in blue whereas the main chain negative charges are shown in red. Lipid-like molecules are shown as red ball-sticks. The red straight line represents a poly-anionic molecule. A) The formation of a prion proceeds through the acquisition of structure within the b-prone-prone 90-145 region as well as partial or total refolding of the C-terminal region that is further stabilized by interaction with lipid-like molecules. This intermediate-like state makes the whole particle highly insoluble causing rapid aggregation. Aliphatic chain interactions arranged in a layer-like fashion on the surface of the prion further stabilize the complex. B) Large complexes of lipid-stabilized misfolded PrP are broken into smaller seeds upon shredding forces such as sonication. The seeds can therefore expose hidden positive charges that are attracted by poly-anionic molecules along with the positives charges of monomeric, native PrP. This bi-dimensional molecular encounters accelerate incorporation of new monomers into the seeds and causes propagation *in vitro*.

GLOSSARY

$(N(CH_3)_4)_2SO_4$	tetramethylammonium sulfate
1X	1 volume
3D	tridimensional
A.U.	arbitrary units
C	Celsius degrees
Cf	co-factor molecule
cm	centimeters
Cu^{+2}	copper ions
Da	Dalton
dG	free energy change
dH	enthalpy change
DNA	deoxyribonucleic acid
dS	entropy change
EDTA	di-sodium ethylenediamine tetra-acetic acid
FTIR	Fourier transform infrared spectroscopy
GdnCl	Carbamimidoylazanium chloride (guanidine hydrochloride)
GPI	Glycosylphosphatidylinositol
HCl	hydrochloride acid
Hepes	2-[4-(2-hydroxyethyl)piperazin-1-yl]ethanesulfonic acid
hrs	hours
IPTG	isopropyl a-D-thiogalactopyranoside
kDa	kilo-Dalton
Kf	statistical weight of the folded fraction
kV	kilo-Volt
lnKf	natural log of Kf

M	Molar
mAb	monoclonal antibody
mg	milligrams
min	minutes
mL	milliliters
mM	milimolar
$N(CH_3)_4Cl$	tetramethylammonium chloride
N2A	neuroblastome cells
Na_2HPO_4	Sodium phosphate buffer
NaCl	sodium chloride
NaF	sodium fluoride
NH_3	amino termini
NH_4F	ammonium fluoride
nm	nanometers
nM	nanomolar
NMR	nuclear magnetic resonance
OD	optical density
PBS	phosphate-buffer saline
PCR	polymerase chain reaction
PK	proteinase-K
PMCA	protein misfolding cyclic amplification
PrP	prion protein
PrP^C	brain-derived prion protein
PrPres	protease-resistant prion protein
PrP^{Sc}	infectious misfolded PrP
recPrP	recombinant prion protein
recPrPres	protease-resistant recombinant prion protein

RNA	ribonucleic acid
rpm	revolutions per minute
SDS	sodium dodecyl sulfate
SDS-PAGE	sodium dodecyl sulfate polyacrylamide gel electrophoresis
SSE	Secondary Structure Estimation
TEM	transmission electron microscopy
Th-T	thioflavin T
Tris	2-Amino-2-hydroxymethyl-propane-1,3-diol
TSE	transmissible spongiform encephalopaties
U/mL	units per milliliter
ug	micrograms
uL	microliter
uM	micromolar
v/v	volume/volume percentage
WB	western-blotting
x g	g-force

BIBLIOGRAPHY

1. Plummer PJ. Scrapie-A Disease of Sheep: A Review of the literature. Can J Comp Med Vet Sci 1946; 10:49-54.

2. Gajdusek DC, Zigas V. Degenerative disease of the central nervous system in New Guinea; the endemic occurrence of kuru in the native population. N Engl J Med 1957; 257:974-978.

3. Gibbons RA, Hunter GD. Nature of the scrapie agent. Nature 1967; 215:1041-1043.

4. Griffith JS. Self-replication and scrapie. Nature 1967; 215:1043-1044.

5. McKinley MP, Bolton DC, Prusiner SB. A protease-resistant protein is a structural component of the scrapie prion. Cell 1983; 35:57-62.

6. Prusiner SB. Novel proteinaceous infectious particles cause scrapie. Science 1982; 216:136-144.

7. Bueler H, Aguzzi A, Sailer A, Greiner RA, Autenried P, Aguet M, et al. Mice devoid of PrP are resistant to scrapie. Cell 1993; 73:1339-1347.

8. Kitamoto T, Tateishi J, Tashima T, Takeshita I, Barry RA, DeArmond SJ, et al. Amyloid plaques in Creutzfeldt-Jakob disease stain with prion protein antibodies. Ann Neurol 1986; 20:204-208.

9. Kitamoto T, Tateishi J, Hikita K, Nagara H, Takeshita I. A new method to classify amyloid fibril proteins. Acta Neuropathol 1985; 67:272-278.

10. Shirahama T, Cohen AS. Structure of amyloid fibrils after negative staining and high-resolution electron microscopy. Nature 1965; 206:737-738.

11. Jimenez JL, Guijarro JI, Orlova E, Zurdo J, Dobson CM, Sunde M, et al. Cryo-electron microscopy structure of an SH3 amyloid fibril and model of the molecular packing. EMBO J 1999; 18:815-821.

12. Chiti F, Webster P, Taddei N, Clark A, Stefani M, Ramponi G, et al. Designing conditions for in vitro formation of amyloid protofilaments and fibrils. Proc Natl Acad Sci U S A 1999; 96:3590-3594.

13. Prusiner SB, McKinley MP, Bowman KA, Bolton DC, Bendheim PE, Groth DF, et al. Scrapie prions aggregate to form amyloid-like birefringent rods. Cell 1983; 35:349-358.

14. Riek R, Hornemann S, Wider G, Billeter M, Glockshuber R, Wuthrich K. NMR structure of the mouse prion protein domain PrP(121-321). Nature 1996; 382:180-182.

15. Caughey B, Raymond GJ. The scrapie-associated form of PrP is made from a cell surface precursor that is both protease- and phospholipase-sensitive. J Biol Chem 1991; 266:18217-18223.

16. Prusiner SB, Scott MR, DeArmond SJ, Cohen FE. Prion protein biology. Cell 1998; 93:337-348.

17. Jarrett JT, Lansbury PT, Jr. Seeding "one-dimensional crystallization" of amyloid: a pathogenic mechanism in Alzheimer's disease and scrapie? Cell 1993; 73:1055-1058.

18. Dobson CM. Protein misfolding, evolution and disease. Trends Biochem Sci 1999; 24:329-332.

19. Fraser H, Dickinson AG. Scrapie in mice. Agent-strain differences in the distribution and intensity of grey matter vacuolation. J Comp Pathol 1973; 83:29-40.

20. Kimberlin RH, Walker CA. Evidence that the transmission of one source of scrapie agent to hamsters involves separation of agent strains from a mixture. J Gen Virol 1978; 39:487-496.

21. Morales R, Abid K, Soto C. The prion strain phenomenon: molecular basis and unprecedented features. Biochim Biophys Acta 2007; 1772:681-691.

22. Outram GW. The pathogenesis of scrapie in mice. Front Biol 1976; 44:325-357.

23. Eklund CM, Kennedy RC, Hadlow WJ. Pathogenesis of scrapie virus infection in the mouse. J Infect Dis 1967; 117:15-22.

24. DeArmond SJ, Yang SL, Lee A, Bowler R, Taraboulos A, Groth D, et al. Three scrapie prion isolates exhibit different accumulation patterns of the prion protein scrapie isoform. Proc Natl Acad Sci U S A 1993; 90:6449-6453.

25. Prusiner SB, Groth DF, Bolton DC, Kent SB, Hood LE. Purification and structural studies of a major scrapie prion protein. Cell 1984; 38:127-134.

26. Bessen RA, Marsh RF. Distinct PrP properties suggest the molecular basis of strain variation in transmissible mink encephalopathy. J Virol 1994; 68:7859-7868.

27. Chien P, Weissman JS, DePace AH. Emerging principles of conformation-based prion inheritance. Annu Rev Biochem 2004; 73:617-656.

28. Weissmann C. A 'unified theory' of prion propagation. Nature 1991; 352:679-683.

29. Manuelidis L, Sklaviadis T, Manuelidis EE. Evidence suggesting that PrP is not the infectious agent in Creutzfeldt-Jakob disease. EMBO J 1987; 6:341-347.

30. Manuelidis L, Sklaviadis T, Akowitz A, Fritch W. Viral particles are required for infection in neurodegenerative Creutzfeldt-Jakob disease. Proc Natl Acad Sci U S A 1995; 92:5124-5128.

31. Muramoto T, Kitamoto T, Hoque MZ, Tateishi J, Goto I. Species barrier prevents an abnormal isoform of prion protein from accumulating in follicular dendritic cells of mice with Creutzfeldt-Jakob disease. J Virol 1993; 67:6808-6810.

32. Prusiner SB. Genetic and infectious prion diseases. Arch Neurol 1993; 50:1129-1153.

33. Saborio GP, Permanne B, Soto C. Sensitive detection of pathological prion protein by cyclic amplification of protein misfolding. Nature 2001; 411:810-813.

34. Castilla J, Saa P, Hetz C, Soto C. In vitro generation of infectious scrapie prions. Cell 2005; 121:195-206.

35. Makarava N, Kovacs GG, Bocharova O, Savtchenko R, Alexeeva I, Budka H, et al. Recombinant prion protein induces a new transmissible prion disease in wild-type animals. Acta Neuropathol 2010; 119:177-187.

36. Legname G, Baskakov IV, Nguyen HO, Riesner D, Cohen FE, DeArmond SJ, et al. Synthetic mammalian prions. Science 2004; 305:673-676.

37. Wang F, Wang X, Yuan CG, Ma J. Generating a prion with bacterially expressed recombinant prion protein. Science 2010; 327:1132-1135.

38. Atarashi R, Moore RA, Sim VL, Hughson AG, Dorward DW, Onwubiko HA, et al. Ultrasensitive detection of scrapie prion protein using seeded conversion of recombinant prion protein. Nat Methods 2007; 4:645-650.

39. Kim JI, Cali I, Surewicz K, Kong Q, Raymond GJ, Atarashi R, et al. Mammalian prions generated from bacterially expressed prion protein in the absence of any mammalian cofactors. J Biol Chem 2010; 285:14083-14087.

40. Diaz-Espinoza R, Soto C. Generation of prions in vitro and the protein-only hypothesis. Prion 2010; 4:53-59.

41. Soto C. Prion hypothesis: the end of the controversy? Trends Biochem Sci 2010; 36:151-158.

42. Tycko R. Solid-state NMR as a probe of amyloid fibril structure. Curr Opin Chem Biol 2000; 4:500-506.

43. Tycko R, Savtchenko R, Ostapchenko VG, Makarava N, Baskakov IV. The alpha-Helical C-Terminal Domain of Full-Length Recombinant PrP Converts to an In-Register Parallel beta-Sheet Structure in PrP Fibrils: Evidence from Solid State Nuclear Magnetic Resonance. Biochemistry 2010; 49:9488-9497.

44. Atarashi R, Wilham JM, Christensen L, Hughson AG, Moore RA, Johnson LM, et al. Simplified ultrasensitive prion detection by recombinant PrP conversion with shaking. Nat Methods 2008; 5:211-212.

45. Supattapone S. Biochemistry. What makes a prion infectious? Science 2010; 327:1091-1092.

46. Swietnicki W, Morillas M, Chen SG, Gambetti P, Surewicz WK. Aggregation and fibrillization of the recombinant human prion protein huPrP90-231. Biochemistry 2000; 39:424-431.

47. Baskakov IV, Legname G, Baldwin MA, Prusiner SB, Cohen FE. Pathway complexity of prion protein assembly into amyloid. J Biol Chem 2002; 277:21140-21148.

48. Baskakov I, Disterer P, Breydo L, Shaw M, Gill A, James W, et al. The presence of valine at residue 129 in human prion protein accelerates amyloid formation. FEBS Lett 2005; 579:2589-2596.

49. Bocharova OV, Breydo L, Parfenov AS, Salnikov VV, Baskakov IV. In vitro conversion of full-length mammalian prion protein produces amyloid form with physical properties of PrP(Sc). J Mol Biol 2005; 346:645-659.

50. Morillas M, Vanik DL, Surewicz WK. On the mechanism of alpha-helix to beta-sheet transition in the recombinant prion protein. Biochemistry 2001; 40:6982-6987.

51. Post K, Pitschke M, Schafer O, Wille H, Appel TR, Kirsch D, et al. Rapid acquisition of beta-sheet structure in the prion protein prior to multimer formation. Biol Chem 1998; 379:1307-1317.

52. Nandi PK, Bera A, Sizaret PY. Osmolyte trimethylamine N-oxide converts recombinant alpha-helical prion protein to its soluble beta-structured form at high temperature. J Mol Biol 2006; 362:810-820.

53. Torrent J, Alvarez-Martinez MT, Harricane MC, Heitz F, Liautard JP, Balny C, et al. High pressure induces scrapie-like prion protein misfolding and amyloid fibril formation. Biochemistry 2004; 43:7162-7170.

54. Sim VL, Caughey B. Ultrastructures and strain comparison of under-glycosylated scrapie prion fibrils. Neurobiol Aging 2009; 30:2031-2042.

55. Caughey B, Baron GS, Chesebro B, Jeffrey M. Getting a grip on prions: oligomers, amyloids, and pathological membrane interactions. Annu Rev Biochem 2009; 78:177-204.

56. Wang F, Yang F, Hu Y, Wang X, Jin C, Ma J. Lipid interaction converts prion protein to a PrPSc-like proteinase K-resistant conformation under physiological conditions. Biochemistry 2007; 46:7045-7053.

57. Jain S, Udgaonkar JB. Salt-induced modulation of the pathway of amyloid fibril formation by the mouse prion protein. Biochemistry 2010; 49:7615-7624.

58. Yeh V, Broering JM, Romanyuk A, Chen B, Chernoff YO, Bommarius AS. The Hofmeister effect on amyloid formation using yeast prion protein. Protein Sci 2009.

59. Sikkink LA, Ramirez-Alvarado M. Salts enhance both protein stability and amyloid formation of an immunoglobulin light chain. Biophys Chem 2008; 135:25-31.

60. Grudzielanek S, Jansen R, Winter R. Solvational tuning of the unfolding, aggregation and amyloidogenesis of insulin. J Mol Biol 2005; 351:879-894.

61. Apetri AC, Surewicz WK. Atypical effect of salts on the thermodynamic stability of human prion protein. J Biol Chem 2003; 278:22187-22192.

62. Peretz D, Williamson RA, Matsunaga Y, Serban H, Pinilla C, Bastidas RB, et al. A conformational transition at the N terminus of the prion protein features in formation of the scrapie isoform. J Mol Biol 1997; 273:614-622.

63. Williamson RA, Peretz D, Pinilla C, Ball H, Bastidas RB, Rozenshteyn R, et al. Mapping the prion protein using recombinant antibodies. J Virol 1998; 72:9413-9418.

64. Bendheim PE, Barry RA, DeArmond SJ, Stites DP, Prusiner SB. Antibodies to a scrapie prion protein. Nature 1984; 310:418-421.

65. Rogers DR. Screening for Amyloid with the Thioflavin-T Fluorescent Method. Am J Clin Pathol 1965; 44:59-61.

66. Forloni G, Angeretti N, Chiesa R, Monzani E, Salmona M, Bugiani O, et al. Neurotoxicity of a prion protein fragment. Nature 1993; 362:543-546.

67. Singh N, Gu Y, Bose S, Kalepu S, Mishra RS, Verghese S. Prion peptide 106-126 as a model for prion replication and neurotoxicity. Front Biosci 2002; 7:a60-71.

68. Chiti F, Dobson CM. Amyloid formation by globular proteins under native conditions. Nat Chem Biol 2009; 5:15-22.

69. Nishina K, Jenks S, Supattapone S. Ionic strength and transition metals control PrPSc protease resistance and conversion-inducing activity. J Biol Chem 2004; 279:40788-40794.

70. Colby DW, Giles K, Legname G, Wille H, Baskakov IV, DeArmond SJ, et al. Design and construction of diverse mammalian prion strains. Proc Natl Acad Sci U S A 2009; 106:20417-20422.

71. Benetti F, Legname G. De novo mammalian prion synthesis. Prion 2009; 3.

72. Deleault NR, Lucassen RW, Supattapone S. RNA molecules stimulate prion protein conversion. Nature 2003; 425:717-720.

73. Deleault NR, Harris BT, Rees JR, Supattapone S. Formation of native prions from minimal components in vitro. Proc Natl Acad Sci U S A 2007; 104:9741-9746.

74. Caughey B. Protease-resistant PrP accumulation and scrapie agent replication: a role for sulphated glycosaminoglycans? Biochem Soc Trans 1994; 22:163-167.

75. Silva JL, Gomes MP, Vieira TC, Cordeiro Y. PrP interactions with nucleic acids and glycosaminoglycans in function and disease. Front Biosci 2010; 15:132-150.

76. Gomes MP, Cordeiro Y, Silva JL. The peculiar interaction between mammalian prion protein and RNA. Prion 2008; 2:64-66.

77. Silva JL, Lima LM, Foguel D, Cordeiro Y. Intriguing nucleic-acid-binding features of mammalian prion protein. Trends Biochem Sci 2008; 33:132-140.

78. Geoghegan JC, Valdes PA, Orem NR, Deleault NR, Williamson RA, Harris BT, et al. Selective incorporation of polyanionic molecules into hamster prions. J Biol Chem 2007; 282:36341-36353.

79. Prusiner SB. Prions. Proc Natl Acad Sci U S A 1998; 95:13363-13383.

80. Prusiner SB, Gabizon R, McKinley MP. On the biology of prions. Acta Neuropathol 1987; 72:299-314.

81. Prusiner SB. Prions are novel infectious pathogens causing scrapie and Creutzfeldt-Jakob disease. Bioessays 1986; 5:281-286.

82. Weissmann C, Bueler H, Fischer M, Sailer A, Aguzzi A, Aguet M. PrP-deficient mice are resistant to scrapie. Ann N Y Acad Sci 1994; 724:235-240.

83. Wang F, Wang X, Yuan CG, Ma J. Generating a Prion with Bacterially Expressed Recombinant Prion Protein. Science 2010; 327:1132-1135.

84. Nordstedt C, Naslund J, Tjernberg LO, Karlstrom AR, Thyberg J, Terenius L. The Alzheimer A beta peptide develops protease resistance in association with its polymerization into fibrils. J Biol Chem 1994; 269:30773-30776.

85. Soto C, Castano EM. The conformation of Alzheimer's beta peptide determines the rate of amyloid formation and its resistance to proteolysis. Biochem J 1996; 314 (Pt 2):701-707.

86. Malisauskas M, Weise C, Yanamandra K, Wolf-Watz M, Morozova-Roche L. Lability landscape and protease resistance of human insulin amyloid: a new insight into its molecular properties. J Mol Biol 2010; 396:60-74.

87. Barry RA, McKinley MP, Bendheim PE, Lewis GK, DeArmond SJ, Prusiner SB. Antibodies to the scrapie protein decorate prion rods. J Immunol 1985; 135:603-613.

88. Bolton DC, McKinley MP, Prusiner SB. Molecular characteristics of the major scrapie prion protein. Biochemistry 1984; 23:5898-5906.

89. Supattapone S, Bosque P, Muramoto T, Wille H, Aagaard C, Peretz D, et al. Prion protein of 106 residues creates an artifical transmission barrier for prion replication in transgenic mice. Cell 1999; 96:869-878.

90. Peretz D, Williamson RA, Legname G, Matsunaga Y, Vergara J, Burton DR, et al. A change in the conformation of prions accompanies the emergence of a new prion strain. Neuron 2002; 34:921-932.

91. Wang F, Yin S, Wang X, Zha L, Sy MS, Ma J. Role of the highly conserved middle region of prion protein (PrP) in PrP-lipid interaction. Biochemistry 2010; 49:8169-8176.

92. Leffers KW, Wille H, Stohr J, Junger E, Prusiner SB, Riesner D. Assembly of natural and recombinant prion protein into fibrils. Biol Chem 2005; 386:569-580.

93. Smirnovas V, Kim JI, Lu X, Atarashi R, Caughey B, Surewicz WK. Distinct structures of scrapie prion protein (PrPSc)-seeded versus spontaneous recombinant prion protein fibrils revealed by hydrogen/deuterium exchange. J Biol Chem 2009; 284:24233-24241.

94. Deleault NR, Geoghegan JC, Nishina K, Kascsak R, Williamson RA, Supattapone S. Protease-resistant prion protein amplification reconstituted with partially purified substrates and synthetic polyanions. J Biol Chem 2005; 280:26873-26879.

95. Edgeworth JA, Jackson GS, Clarke AR, Weissmann C, Collinge J. Highly sensitive, quantitative cell-based assay for prions adsorbed to solid surfaces. Proc Natl Acad Sci U S A 2009; 106:3479-3483.

96. Zobeley E, Flechsig E, Cozzio A, Enari M, Weissmann C. Infectivity of scrapie prions bound to a stainless steel surface. Mol Med 1999; 5:240-243.

97. Weber P, Giese A, Piening N, Mitteregger G, Thomzig A, Beekes M, et al. Cell-free formation of misfolded prion protein with authentic prion infectivity. Proc Natl Acad Sci U S A 2006; 103:15818-15823.

98. Wille H, Michelitsch MD, Guenebaut V, Supattapone S, Serban A, Cohen FE, et al. Structural studies of the scrapie prion protein by electron crystallography. Proc Natl Acad Sci U S A 2002; 99:3563-3568.

99. Govaerts C, Wille H, Prusiner SB, Cohen FE. Evidence for assembly of prions with left-handed beta-helices into trimers. Proc Natl Acad Sci U S A 2004; 101:8342-8347.

100. DeMarco ML, Daggett V. From conversion to aggregation: protofibril formation of the prion protein. Proc Natl Acad Sci U S A 2004; 101:2293-2298.

101. Dorosz J, Volinsky R, Bazar E, Kolusheva S, Jelinek R. Phospholipid-induced fibrillation of a prion amyloidogenic determinant at the air/water interface. Langmuir 2009; 25:12501-12506.

102. Tsiroulnikov K, Shchutskaya Y, Muronetz V, Chobert JM, Haertle T. Phospholipids influence the aggregation of recombinant ovine prions. From rapid extensive aggregation to amyloidogenic conversion. Biochim Biophys Acta 2009; 1794:506-511.

103. Re F, Sesana S, Barbiroli A, Bonomi F, Cazzaniga E, Lonati E, et al. Prion protein structure is affected by pH-dependent interaction with membranes: a study in a model system. FEBS Lett 2008; 582:215-220.

104. Sanghera N, Swann MJ, Ronan G, Pinheiro TJ. Insight into early events in the aggregation of the prion protein on lipid membranes. Biochim Biophys Acta 2009; 1788:2245-2251.

105. Gale P. The prion/lipid hypothesis--further evidence to support the molecular basis for transmissible spongiform encephalopathy risk assessment. J Appl Microbiol 2007; 103:2033-2045.

106. Notari S, Strammiello R, Capellari S, Giese A, Cescatti M, Grassi J, et al. Characterization of truncated forms of abnormal prion protein in Creutzfeldt-Jakob disease. J Biol Chem 2008; 283:30557-30565.

107. Bocharova OV, Breydo L, Salnikov VV, Gill AC, Baskakov IV. Synthetic prions generated in vitro are similar to a newly identified subpopulation of PrPSc from sporadic Creutzfeldt-Jakob Disease. Protein Sci 2005; 14:1222-1232.

108. Zou WQ, Capellari S, Parchi P, Sy MS, Gambetti P, Chen SG. Identification of novel proteinase K-resistant C-terminal fragments of PrP in Creutzfeldt-Jakob disease. J Biol Chem 2003; 278:40429-40436.

109. Wille H, Bian W, McDonald M, Kendall A, Colby DW, Bloch L, et al. Natural and synthetic prion structure from X-ray fiber diffraction. Proc Natl Acad Sci U S A 2009; 106:16990-16995.

110. Zahn R, Liu A, Luhrs T, Riek R, von Schroetter C, Lopez Garcia F, et al. NMR solution structure of the human prion protein. Proc Natl Acad Sci U S A 2000; 97:145-150.

111. Lansbury PT. Mechanism of scrapie replication. Science 1994; 265:1510.

112. Tagliavini F, Prelli F, Verga L, Giaccone G, Sarma R, Gorevic P, et al. Synthetic peptides homologous to prion protein residues 106-147 form amyloid-like fibrils in vitro. Proc Natl Acad Sci U S A 1993; 90:9678-9682.

113. Selvaggini C, De Gioia L, Cantu L, Ghibaudi E, Diomede L, Passerini F, et al. Molecular characteristics of a protease-resistant, amyloidogenic and neurotoxic peptide homologous to residues 106-126 of the prion protein. Biochem Biophys Res Commun 1993; 194:1380-1386.

114. Nandi PK. Polymerization of human prion peptide HuPrP 106-126 to amyloid in nucleic acid solution. Arch Virol 1998; 143:1251-1263.

115. Zheng W, Wang L, Hong Y, Sha Y. PrP106-126 peptide disrupts lipid membranes: influence of C-terminal amidation. Biochem Biophys Res Commun 2009; 379:298-303.

116. Zhang Y, Zhao X, Wang PY. Molecular dynamics study of the fibril elongation of the prion protein fragment PrP106-126. J Theor Biol 2007; 245:238-242.

117. Colby DW, Wain R, Baskakov IV, Legname G, Palmer CG, Nguyen HO, et al. Protease-sensitive synthetic prions. PLoS Pathog 2010; 6:e1000736.

118. Piro JR, Harris BT, Supattapone S. In situ photodegradation of incorporated polyanion does not alter prion infectivity. PLoS Pathog 2011; 5:e1002001.

VITA

Rodrigo Carlos Diaz Espinoza was born on October 21st, 1979, Santiago, Chile. All his primary and secondary education was carried in Liceo Experimental Manuel de Salas, Santiago. In 1998, he was accepted in first place to start college studies in the Universidad de Chile, pursuing a major in Molecular Biotechnology Engineering. In 2004, he obtained the Bachelor of Sciences degree, ranking first among 33 students. After conducting his undergraduate thesis work under Dr. Octavio Monasterio mentoring, which was published later in 2007, Rodrigo obtained the Engineer degree in 2005, with *summa cum laude* honor. During his undergraduate studies, he presented his work in several national meetings. In 2004, he received a fellowship for a one-month rotation at the Universidad Federal de Minas Gerais, Brazil, under the guidance of Dr. Marcelo Santoro. In 2005, he joined The University of Texas Medical Branch, USA, to pursue graduate studies in the Molecular Biophysics PhD Program. There, he rotated in three different labs conducted by: Dr. Andres Oberhauser, Dr. Vincent Hilser and Dr Wayne Bolen (under Dr. Joerg Roesgen mentoring). In 2006, he joined Dr. Claudio Soto's lab to continue his PhD thesis work. Rodrigo has presented his graduate research in several national and international meetings, such as The Gibbs Conference (Illinois, USA, 2009) and Prion Meeting (Madrid, Spain, 2008).

Publications

1. Diaz-Espinoza R, Mukherjee A, Soto, C. Kosmotropic anions convert recombinant prion protein into a PrPSc-like misfolded isoform (submitted to Journal of Biological Chemistry).
2. Diaz-Espinoza R, Soto C. Generations of prions and the protein-only hypothesis. Prion 2010; 4:53-59.

3. Morales R, Estrada LD, Diaz-Espinoza R, Morales-Scheihing D, Jara MC, Castilla J, Soto C. Molecular cross talk between misfodled proteins in animal models of Alzheimer's and prion diseases. J Neurosci 2009; 30:4528-4530.
4. Banks WA, Robinson SM, Diaz-Espinoza R, Urayama A, Soto C. Transport of prion protein across the blood-brain barrier. Exp. Neurol 2009;18:162-167.
5. Díaz-Espinoza R, Garcés AP, Arbildua JJ, Montecinos F, Brunet JE, Lagos R, Monasterio O. Domain folding and flexibility of Escherichia coli FtsZ determined by tryptophan site-directed mutagenesis. Protein Sci 2007;16:1543-1556.

Abstracts

1. Diaz-Espinoza R, Oezguen N, Cattaneo R, Braun W. Determination of the potential receptor binding site of the measles virus haemagglutinin. The Academy of Medicine, Engineering and Science of Texas conference on Bugs, Drugs & Vaccines, Galveston, Texas (April 5-6, 2006).
2. Oezguen N, Diaz-Espinoza R, Cattaneo R, Braun W. 3D model of the complex of measles virus haemagglutinin and its human receptor SLAM". Sealy Center for Structural Biology and Molecular Biophysics 11th Annual Structural Biology Symposium, University of Texas Medical Branch, Galveston, Texas (May 19-20, 2006)
3. Fuson K, Diaz-Espinoza R, Sutton B, Oberhauser B. The mechanical properties of human Synaptotagmin 1 C2 domains. 51st Annual Meeting of the Biophysical Society, Baltimore, Maryland, (March 3-7, 2007)
4. Diaz-Espinoza R, Whitten S, Morales R, Hilser V, Soto C. Peptide ligands that target the cooperative folding network in the prion protein stimulate PrPres formation. Annual Meeting of the Europrion Society, Madrid, Spain, (October 8-10, 2008)
5. Diaz-Espinoza R, Garces A, Whitten S, Soto C, Hilser V. Denatured-ensemble-based thermodynamic analysis of prion and amyloid sequences". Gibbs Conference, Carbondale, USA, (October 2009).